CADMD 2021

under the patronage of Professor Jerzy Lis AGH UST Rector

Proceedings

of the XXIX International Polish-Ukrainian Conference

“CAD in Machinery Design. Implementation and Educational Issues”

Faculty of Mechanical Engineering and Robotics

AGH University of Science and Technology

Department of Computer Aided Systems

Lviv Polytechnic National University

Faculty of Mechanical Engineering

Bialystok University of Technology

Institute of Machine Design Fundamentals

Warsaw University of Technology

LVIV, 2021

CADMD 2021

under the patronage of Professor Jerzy Lis AGH UST Rector

Proceedings

of the XXIX International Polish-Ukrainian Conference

“CAD in Machinery Design. Implementation and Educational Issues”

Faculty of Mechanical Engineering and Robotics

AGH University of Science and Technology

Department of Computer Aided Systems

Lviv Polytechnic National University

Faculty of Mechanical Engineering

Bialystok University of Technology

Institute of Machine Design Fundamentals

Warsaw University of Technology

LVIV, 2021

XXIX ПОЛЬСЬКО-УКРАЇНСЬКА КОНФЕРЕНЦІЯ
“САПР У ПРОЕКТУВАННІ МАШИН.
ПИТАННЯ ВПРОВАДЖЕННЯ ТА НАВЧАННЯ“

XXIX POLSKO-UKRAIŃSKA KONFERENCJA
“CAD W PROJEKTOWANIU MASZYN.
PROBLEMY WDRAŻANIA I NAUCZANIA”

XXIX POLISH-UKRAINIAN CONFERENCE ON
“CAD IN MACHINERY DESIGN.
IMPLEMENTATION AND EDUCATIONAL ISSUES”

CADMD 2021

Ministry of Education and Science of Ukraine

Lviv Polytechnic National University

CAD in Machinery Design. Implementation and Educational Issues

Proceedings

of the XXIX International Polish-Ukrainian Conference

Under the patronage of Professor
Jerzy Lis AGH UST Rector

9–10 December 2021

Krakow, Poland

Lviv
Lviv Polytechnic Publishing House
2021

Міністерство освіти і науки України
Національний університет «Львівська політехніка».

САПР у проектуванні машин. Питання впровадження та навчання

Матеріали
XXIX Міжнародної польсько-української науково-технічної конференції

Під патронатом ректора Гірничо-металургійної академії імені Станіслава Сташиця професора Єжи Ліса

9-10 грудня 2021

Краків, Польща

Львів
Видавництво Львівської політехніки
2021

УДК 004.896
С197

Організатори конференції

Краківська гірничо-металургійна академія імені Станіслава Сташиця, Польща
Факультет машинобудування та робототехніки
Національний університет "Львівська політехніка", Україна
Кафедра систем автоматизованого проектування Інституту комп'ютерних наук та інформаційних технологій
Білостоцька політехніка, Польща, Факультет машинобудування
Варшавська політехніка, Польща, Інститут основ машинобудування

Organized by

AGH University of Science and Technology, Poland
Faculty of Mechanical Engineering and Robotics,
Lviv Polytechnic National University, Ukraine
Institute of Computer Science and information technologies
Department of Computer Aided Design Systems,
Bialystok University of Technology, Poland, Faculty of Mechanical Engineering,
Warsaw University of Technology, Poland, Institute of Machine Design Fundamentals

САПР у проектуванні машин. Питання впровадження та навчання (CADMD 2021): матеріали XXIX Міжнародної польсько-української конференції під патронатом ректора Гірничо-металургійної академії імені Станіслава Сташиця професора Єжи Ліса.: CADMD 2021. – Львів: Видавництво Львівської політехніки, 2021. – 40 с.
С197
ISBN 978-966-941-686-5

Подано матеріали конференції з проблем у галузі автоматизації проектування машин та механізмів, ідентифікації, моделювання процесів і систем, робототехніки і автоматики, електромеханічних систем, застосування а інформаційних технологій в інженерії, програмного забезпечення, програмування і алгоритмів, інженерних баз даних, інженерної освіти освітніх методик та інтернет технологій у навчанні.

Видання призначене для науковців, аспірантів та студентів старших курсів.

УДК 004.896

Відповідальний за випуск – к. т. н., доцент Здобицький А.Я.

Матеріали подано в авторській редакції

ISBN 978-966-941-685-8

INTERNATIONAL ORGANIZING COMMITTEE

Chairmen:

Prof. Jerzy Lis
AGH UST Rector, Poland,

Prof. Krzysztof Mendrok
AGH University of Science and Technology, Poland

Prof. Mykhailo Lobur
Lviv Polytechnic National University, Ukraine

Prof. Marian Banaś
AGH University of Science and Technology, Poland

Prof. Roman Kaczyński
Białystok University of Technology, Poland

Conference Secretary:

Dr hab. inż. Krzysztof Pytel
AGH University of Science and Technology, Poland

Dr. Andriy Zdobytskyi
Lviv Polytechnic National University, Ukraine

Members of Organizing Committee:

Dr. Andriy Kernytskyy

Dr. Mykhaylo Melnyk

Dr. Uliana Marikutsa

Bsc. Panchyshyn Diana

Bsc. Yuliia Neymet

Lviv Polytechnic National University, Ukraine

INTERNATIONAL PROGRAM COMMITTEE

Prof.	**Mykhailo Lobur**	Lviv Polytechnic National University
Prof.	**Aivars Aboltins**	Latvia University of Life Sciences and Technologies
Prof.	**Marian Banaś**	AGH University of Science and Technology
Prof.	**Roman Kaczyński**	Białystok University of Technology
Prof.	**Jerzy Bajkowski**	Warsaw University of Technology
Prof.	**Anna Timofiejczuk**	Silesian University of Technology
Prof.	**Wojtek Sitek**	Silesian University of Technology
Prof.	**Krzysztof Gaska**	Silesian University of Technology
Prof.	**Bogusław Łasarz**	Silesian University of Technology
Prof.	**Janusz Kotowicz**	Silesian University of Technology
Prof.	**Marek Iwaniec**	AGH University of Science and Technology
Prof.	**Jerzy Józwik**	Lublin University of Technology
Prof.	**Krzysztof Mendrok**	AGH University of Science and Technology
Prof.	**Krzysztof Kołodziejczyk**	AGH University of Science and Technology
Prof.	**Petro Kosobutskyy**	Lviv Polytechnic National University
Prof.	**Piotr Krawiec**	Poznań University of Technology
Prof.	**Tadeusz Kamisiński**	AGH University of Science and Technology
Dr.	**Andrzej Łukaszewicz**	Białystok University of Technology
Prof.	**Oleh Matviykiv**	Lviv Polytechnic National University
Dr.	**Mykhaylo Melnyk**	Lviv Polytechnic National University
Prof.	**Jerzy Pokojski**	Warsaw University of Technology
Prof.	**Krzysztof Pytel**	AGH University of Science and Technology
Prof.	**Dariusz Perkowski**	Białystok University of Technology
Prof.	**Yaroslav Sokolovsky**	Lviv Polytechnic National University
Prof.	**Zinoviy Stotsko**	Lviv Polytechnic National University
Prof	**Tadeusz Telejko**	AGH University of Science and Technology
Prof	**Wiesław Tarełko**	Maritime Academy in Gdynia
Prof	**Robert Zalewski**	Warsaw University of Technology
Prof	**Rafał Wiśniowski**	AGH University of Science and Technology
Prof	**Vladyslav Yevsieiev**	Kharkov National University of Radio Electronics

CONTENT

ANALYSIS OF APPLICABILITY OF FLOW-ACOUSTIC COUPLING USED FOR THE PRESSURE MEASUREMENT

Paweł Łojek[1], Ireneusz Czajka[2]
AGH University of Science and Technology[1]
lojek@agh.edu.pl
AGH University of Science and Technology[2]
iczajka@agh.edu.pl.

ABSTRACT

The paper presents concept and results of initial simulations of acoustic system for absolute pressure measurement. Its working principle is based on coupling between flow and acoustic fields. The measurement is performed indirectly. Measurement of absolute pressure is based on measure of velocity and time of arrival of acoustic wave, and relation between pressure and speed of sound in given medium. Concept was verified numerically using finite volume method and OpenFOAM environment. Example implementation of the system and its measurement uncertainty was also presented. Possible application of the system is to measure mean pressure on the walls of the buildings.

KEYWORDS: **measurement system, numerical simulation, pressure measurement**

I. INTRODUCTION

Knowledge about pressure acting on the walls of the buildings is crucial in design and diagnostics of both new and existing buildings. Currently used methods allow for wind pressure measure using matrix of piezoresistive or piezoelectric sensors. This method are highly inefficient and expensive. The lack of efficient method of measuring pressure acting on buildings was main reason for developing a new method, allowing measurement of mean pressure on given distance.

The problem of measuring nonelectrical values, such as pressure, is connected with developing a sensor capable of registering quantity which is easy to measure and choosing a transducer which allows converting measured signal to electric one. Authors decided to use coupling between thermodynamic state variables and acoustic field parameters. In researched case, coupling between flow and acoustic fields was used.

II. IDEA OF THE MEASUREMENT SYSTEM

The working principle of measurement system is based on linearized Euler equations, time of arrival of acoustic wave and known distance between transducers. The working principle of the system is shown in the Fig 1a. The pressure is obtained by the equation:

$$p = \frac{L^2 \rho}{\kappa t^2} \tag{1}$$

Where: p – pressure, L – distance between transducers, $\varkappa$ - adiabatic index, ρ - density, t – time of arrival of wave.

The main issue that may disturb the system are disturbances caused by the air flow parallel to axis connecting transduces. Influence of movement of medium can change wave velocity. One of the assumptions of the concept was symmetrical distribution of v_y speed component (parallel to the side of the obstacle in the flow, i.e. building wall, (Fig. 1b) The assumption was verified by numerical simulations.

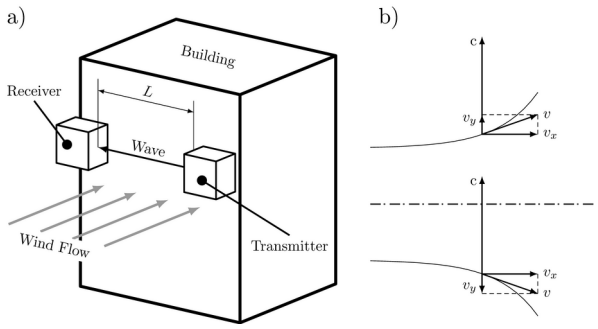

Figure 1: a) possible application of the system for the pressure measurement on elevation of buildings, b) distribution of flow and acoustic wave velocities

III. NUMERICAL SIMULATIONS

Simulations of the flow around cylindrical obstacle were carried out to verify concept described above. Velocity and pressure fields which were results of simulations allowed to verify if influence of moving medium interferes with wave velocity and disrupts the measurement.

The geometric model and computational mesh were created with Salome, open source CAD software, and numerical simulations were performed with finite volume method and OpenFOAM software. Air flow with velocity equal to 5, 10 and 20 m/s was computed. For velocity of 5 m/s , flow at yaw angle equal to 5,10,20, 30 ° was also modeled.

IV. CONCLUSIONS

Numerical simulations showed that concept and the assumptions of the measurement system are correct. Prototype of measurement system was also designed and assembled. Measurements carried out using it have shown that pressure can be measured using flow-acoustic coupling.

The next stage of building the measurement system will be the development of new model that takes coupling of acoustic and flow fields into account. Experimental verification of simulations of the flow around obstacle in wind tunnels are necessary. Prototype of the system has to be rebuild using more accurate components.

ANALYSIS OF THE EXTERNAL FACTORS INFLUENCING THE AVAILABILITY AND POWER OF GAS ENGINES

Adam Kalwar[1], Krzysztof Pytel[2], Franciszek Kurdziel[1], Grzegorz Grzywnowicz[1], Uliana Marikutsa [3]
PGNiG Termika Energetyka Przemysłowa S.A., Jastrzębie Zdrój[1]
kalwar@agh.edu.pl
AGH University of Science and Technology[2]
kpytel@agh.edu.pl
Lviv Polytechnic National University[3]
Uliana.B.Marikutsa@lpnu.ua

ABSTRACT

This study presents the factors that have a direct impact on the operation of gas combustion engines - used in power generators connected to the power grid. Factors hindering the operation, methods of solving problems at the stage of operation will be presented, as well as conclusions for the future that can be used in subsequent projects of cogeneration installations.

KEYWORDS: **power systems, environmental protection facilities, process control, computer applications in engineering**

I. INTRODUCTION

This study analyzes the operating conditions of gas engines fueled with mine gas, installed on the site of the former mine. This location also has a specific impact on the efficiency of work and specific activities that must be performed for the engines to work without failure.

II. IMPACT OF SELECTED FACTORS ON ENGINE OPERATION

Gas engines need certain conditions, the fulfillment of which enables the achievement of the assumed efficiency parameters as well as the planned power, both electric and thermal power for their trouble-free operation [1]. Due to the location, the direction of the wind has a significant influence on the amount of pollution, in this area there are often winds blowing from the direction of the coal storage yard towards the gas engine buildings. The phenomenon of fouling of air handling units' filters intensifies during periods of drought, as well as during the period of coal supply to the dump, as well as during the operation of the dump, i.e. during the carburizing of boilers.

During the operation of the gas engine, it was also found that the combustion air filters become dirty very quickly. Contamination of combustion air filters was sometimes very quick, sometimes they had to be replaced every 250 person-hours. The phenomenon seemed mysterious because the engine building is closed and tight, and the air-handling units already described are responsible for supplying combustion air. During subsequent cases of premature contamination of the combustion air filters, the degree of contamination of the filters of the air-handling units was also checked. During these inspections, it turned out that despite the contamination of the combustion air filters, the filters of the air-handling units remain in a condition that does not require replacement.

Gas engines operate during the heating season with the maximum load of the heat recovery system, the heat is transferred through the plate exchanger to the heating system, thus relieving the engine cooling system. This state usually lasts from September to May. After this period, the heat is transferred to the heating network to a limited extent, additionally, increasing ambient temperatures cause an increasing load on the engine cooling system. The engine cooling system without heat recovery is designed to maintain maximum engine efficiency at an ambient temperature of 30°C. The diagram of the load changes of the engine heat recovery system is presented in Fig. 1. The orange line shows the amount of heat energy production in domestic hot water, while the turquoise line is the production of heat energy for central heating.

Fig. 1. Changes in thermal power transferred to the heating network in the year

III. SUMMARY

The availability of a gas engine is influenced by the amount of available gas, breakdowns and service inspections. Engine power availability depends on, the amount of available gas, gas parameters, the technical condition of the engine and the amount of heat reception depending on the outside temperature. Some of the factors that affect the availability of a gas engine can be influenced, others cannot be influenced and it must be assumed that this is the nature of the installation. The optimal work system for a gas engine would be work with year-round heat removal

REFERENCES

[1] M. J. Moran, H. N. Shapiro, D. D. Boettner, and M. B. Bailey, Fundamentals of engineering thermodynamics. Eighth edition. John Wiley & Sons, Inc, 2014, pp. 509-562.

ANALYSIS OF THE OPERATIONAL PROBLEMS OF METHANE ENERGY FUEL

Adam Kalwar[1], Krzysztof Pytel[2], Franciszek Kurdziel[1], Grzegorz Grzywnowicz[1], Mykhailo Melnyk[3]
PGNiG Termika Energetyka Przemysłowa S.A., Jastrzębie Zdrój[1]
kalwar@agh.edu.pl
AGH University of Science and Technology[2]
kpytel@agh.edu.pl
Lviv Polytechnic National University[3]
Mykhaylo.R.Melnyk@lpnu.ua

ABSTRACT

The aim of this work is to present the issues related to the operation of cogeneration units powered by gas engines using mine gas as fuel. Gas engines are more and more often used to drive electric generators, in this application gas is used as fuel, be it coke oven, septic gas, network natural gas or mine. In the area where coal is mined, mine gas is commonly used as fuel to power cogeneration units. The use of mine gas as fuel is highly desirable for ecological and economic reasons. In this study, the advantages and difficulties of using this gas as a fuel will be presented.

KEYWORDS: **power systems, environmental protection facilities, process control, computer applications in engineering**

I. INTRODUCTION

Methane is perceived as a factor increasing the already great threat to the work of miners extracting hard coal. Due to the need to increase work safety, the mines extract methane to the surface in such a quantity as to ensure relatively safe working conditions underground. For years, attempts have been made in mines to burn gas in energy devices. The publication will present mine gas not as an environmental pollutant - when blown into the atmosphere, not as an unwanted by-product of coal mining, but as a good energy fuel. The advantages, disadvantages and potential directions of development in the use of methane in the energy sector will be presented.

II. GAS PARAMETERS ANALYSIS

From the beginning of the operation of the analyzed gas network, the mixture composition was monitored only in terms of pure CH4 concentration in the mixture. The content of methane in the mixture was measured with stationary methane meters at mine methane drainage stations and at individual plants consuming mine gas. Additionally, in each plant, three times a day, and more often if necessary, the content of CH4 in the mixture was measured with manual methane meters. The procedure of measuring the concentration with a personal methane meter has been carried out until now. For several years, the composition of the gas has been monitored non-stop at individual intakes and receipts by means of chromatographs. This solution makes it possible to very accurately determine the quality of the gas and the variability of its composition, at any time horizon [1].

When analyzing the results, it can be seen that a large concentration difference of up to 30% does not significantly affect the quality of gas in the source, where the average concentration in 2019 was 54.3%. The shots that have a decisive impact on the quality of the mixture supplied as fuel for gas engines were selected for the analysis. Fig. 1 shows that the maximum concentration of the selected shot is quite stable and amounts to about 70%, while the minimum concentration of the shot is significantly lower and has greater variability. However, it can be assumed that such changes in concentration in both intakes are significantly influenced by the exploitation of coal deposits.

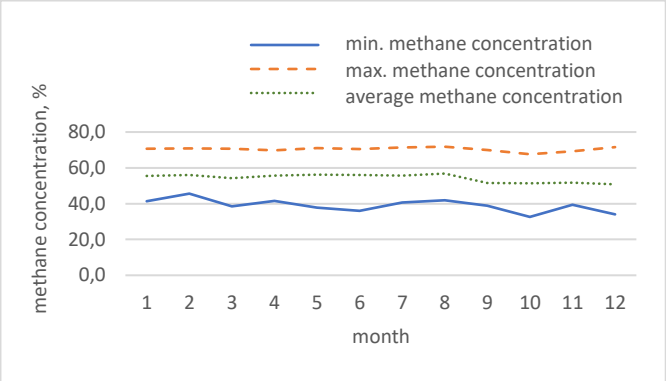

Fig. 1. Changes in methane concentration in the year

Changes in the gas concentration on the engine supply do not have a significant impact on the operation of the gas engine; the engine control system copes quickly and efficiently with the engine overshoot and maintaining the set power. Certainly, the combination of several gas supply sources has a positive effect on the stable operation of the entire gas network, there are no frequent and rapid changes in concentration, if such situations occur, and these are purely emergency cases.

III. SUMMARY

Mine gas is quite a good fuel for electro-energy devices, but a extensive technical infrastructure is required, thanks to which it can be managed in an optimal way.

REFERENCES

[1] M. J. Moran, H. N. Shapiro, D. D. Boettner, and M. B. Bailey, Fundamentals of engineering thermodynamics. Eighth edition. John Wiley & Sons, Inc, 2014, pp. 509-562.

ANALYSIS OF THE PROCESSES TAKING PLACE IN THE ABSORBER OF AN ABSORPTION CHILLER

Franciszek Kurdziel[1], Krzysztof Pytel[2], Adam Kalwar[1], Grzegorz Grzywnowicz[1], Andriy Zdobytskyi[3], Jastrzębie Zdrój[1]
PGNiG Termika Energetyka Przemysłowa S.A.[1]
kurdziel@agh.edu.pl
AGH University of Science and Technology[2]
kpytel@agh.edu.pl
Lviv Polytechnic National University[3]
andrii.y.zdobytskyi@lpnu.ua

ABSTRACT

The article presents the ways of using absorption chillers, based on the example of a mine air-conditioning system. The paper presents the application of the possibility of using thermal energy as a waste product resulting from the combustion of gas (methane; CH4) in gas engines, and the process of its processing into the production of a cooling medium. The principles of operation of an absorption chiller are described - the processes in the absorber, physicochemical changes in the system and the method of producing chilled water. The article presents the actual application of cascade-connected refrigeration devices in order to achieve the final product with specific parameters.

KEYWORDS: **power systems, environmental protection facilities, process control, computer applications in engineering**

I. INTRODUCTION

The analyzed combined energy and cooling system consists of several technological lines, built in several stages. Installations were created in such a way that it was possible to increase the cooling capacity in case of increased demand. The first two process lines include a gas engine with an electric power of 3.2 MWe and a thermal power of 3.7 MWt, two absorption chillers and a compressor chiller with a cooling capacity of 2.5 MWch. The total cooling capacity that the system can generate is 5 MWch. In the next stage of construction, a third gas engine was launched with electric and thermal capacity of 3.9 MWe and 4.3 MWt, respectively.

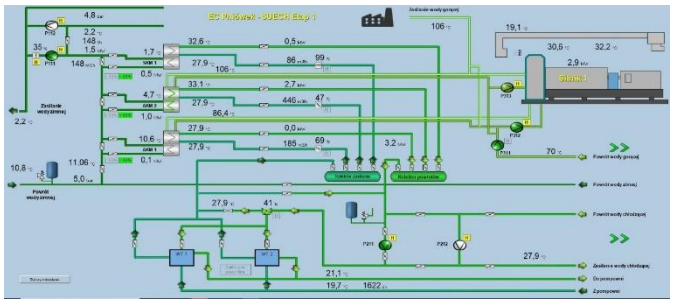

Fig. 1. Cooling system based on heat from a gas engine

The cooling system shown in Fig. 1 is built on the basis of heat recovery from a gas engine - heat recovery system from exhaust gases; heat recovery system from the engine body. The heat exchange between the recovery systems is based on water heat exchangers. The heated water from the waste heat of a gas engine with a temperature of up to 130 ° C is used as an energy source in absorption chillers to produce cold water.

II. OPERATIONAL PROBLEMS DURING THE OPERATION OF A COMPUTER-CONTROLLED SYSTEM

Crystallization may occur in all absorption chillers that use lithium bromide and water as solution and refrigerant. This is because certain concentration levels of the liquid solution in certain areas of the system can only be obtained above the normal ambient temperature [1]. Typically, the solution in the single-stage absorption unit generator has 64.3% lithium bromide (by weight). LiBr solutions start to crystallize at 43.3°C. Crystallization occurs when the temperature of the LiBr solution becomes too low or the concentration is too high. Then the LiBr solution thickens. The LiBr solution cannot then absorb any more water and starts to solidify (crystallize). Crystallization takes place in the heat exchanger.

The case of lithium bromide crystallization in a new absorption refrigerator was considered. The conducted analysis showed periodic exceeding of the recommended operating ranges for several parameters. The most frequent event was that the cold water temperature at the inlet to the device dropped below the acceptable value. Another anomaly was exceeding the nominal hot water flow. This situation could be due to incorrect setting of the maximum opening valve of the hot water regulating valve in the refrigerator controller in such a way that the flow does not exceed the nominal value.

III. SUMMARY

Common engineering practice indicates a set of several steps that are recommended to be performed in order to successfully decrystallize the lithium bromide solution in an absorption chiller. The final sequence and duration of individual activities depends on the place and degree of crystallization. The main activity is forcing the refrigerant from the evaporator of the device to the absorber in order to reduce the concentration of the diluted solution, pumped into the generator.

REFERENCES

[1] M. J. Moran, H. N. Shapiro, D. D. Boettner, and M. B. Bailey, Fundamentals of engineering thermodynamics. Eighth edition. John Wiley & Sons, Inc, 2014, pp. 609-629.

ANALYSIS OF THE PROCESSES TAKING PLACE IN THE ABSORBER OF AN ABSORPTION CHILLER

Franciszek Kurdziel[1], Krzysztof Pytel[2], Adam Kalwar[1], Grzegorz Grzywnowicz[1], Mykhailo Lobur[3], Jastrzębie Zdrój[1]
PGNiG Termika Energetyka Przemysłowa S.A.[1]
kurdziel@agh.edu.pl
AGH University of Science and Technology[2]
kpytel@agh.edu.pl
Lviv Polytechnic National University[3]
Mykhaylo.V.Lobur@lpnu.ua

ABSTRACT

The article presents the characteristics of the operation of a compressor cooler for the needs of cold generation for the central mine air-conditioning system. The methods of operation of devices are described and their use in the final stage of chilled water cooling. The construction of a screw compressor and methods of compression are discussed. The actual application of compressors in the third stage of chilled water production has been presented. The free-cooling installation was presented as a solution supporting the production of cold.

KEYWORDS: **power systems, environmental protection facilities, process control, computer applications in engineering**

I. INTRODUCTION

The ammonia cooling installation of the combined system (Fig. 1) was made to cool the water returning from the mine to a temperature of about + 1.5°C in an integrated cooling unit with ammonia as a working medium. The completed water cooling unit acts as a supplementary system, which will be activated when it is not possible to cool the water to the desired temperature + 1.5°C by the existing free cooling system and the existing absorption-compressor systems.

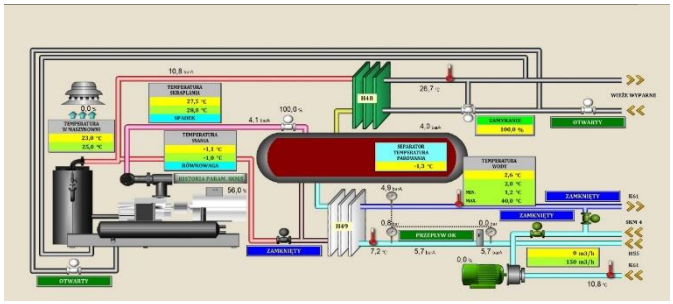

Fig. 1. Installation of a compressor cooler

When the hot water, after passing through the existing absorption cooling systems, is not cooled to the desired temperature, shut-off valves with an actuator should automatically shut off the flow of water to the cold chamber of the mine water pumping system [1]. Then warm water should be directed to the ammonia water cooling system, where the water will be cooled to the desired temperature of + 1.5°C.

II. THE ISSUE OF THE INTERNAL VOLUME RATIO OF THE COMPRESSOR

The operation of the system is fully automatic and fully automatically cooperates with existing free cooling systems and existing absorption-compressor systems. All parameters of the ammonia and water installations (pressures, temperatures, refrigerant levels, operating states of devices, capacities of ammonia compressors and water pumps) are continuously displayed, monitored and archived by a central controller that controls the operation of the entire cooling and water installation.

In screw compressors, as the rotors rotate, the volume of gas sucked in between the main and auxiliary rotors decreases, which causes an increase in pressure. As soon as the gas volume sucked in decreases to the designed volume (internal volume factor), the gas enters the discharge port and is pushed out of the compressor. For screw compressors, the internal volume ratio represents the ratio between the gas volume at the start of the compression process to the gas volume after the end of the compression process. The internal volume ratio is the ratio of the volume between the toothed space of the rotors and the compressor casing after the suction process is complete, and the volume ratio when the discharge port begins to open. On most compressors, internal volume ratio is fixed at 2.63, 3.65, or 5.8.

The solution to the problem is the ability to change the internal volume ratio. The variable internal volume ratio during standstill allows the compressor to be optimally adapted to the load. As a result, one compressor can work efficiently in various pressure ranges.

III. SUMMARY

Compressors with a constant internal volume ratio use energy inefficiently if the internal volume ratio does not match the operating conditions. When a compressor with the high internal volume ratio is operated under low compression ratios - as a result the gas pressure becomes higher than the discharge pressure before reaching the discharge port - this results in a waste of energy which is used for further, unnecessary compression.

REFERENCES

[1] M. J. Moran, H. N. Shapiro, D. D. Boettner, and M. B. Bailey, Fundamentals of engineering thermodynamics. Eighth edition. John Wiley & Sons, Inc, 2014, pp. 190-195.

AUTOMATED 3D DESIGN OF PRINTED CIRCUIT BOARDS IN CAD SOLIDWORKS

Serhii Avdieiev, Tamara Klymkovych, Roman Panchak, Kostyantyn Kolesnyk
serhii.avdieiev.mknm.2020@lpnu.ua, tamara.a.klymkovych@lpnu.ua,
roman.t.panchak@lpnu.ua, kostyantyn.k.kolesnyk@lpnu.ua
Lviv Polytechnic National University

Abstract **- The article presents methods and tools of 3D modeling in CAD SolidWorks and creates a subsystem that would help create printed circuit boards of various sizes, place elements on printed circuit boards, move them using modeling tools, and conduct appropriate thermal analysis.**

KEYWORDS: **components, 3D modeling, SolidWorks, simulation, thermal analysis.**

I. INTRODUCTION AND RESEARCH OBJECTIVE

At the time of computer technology and scientific and technological progress, the use of printed circuit boards for the manufacture of high-tech products (smart devices) has become widely used [1-3].

The most common reason that leads to rapid board failure is overheating. It can occur due to climatic conditions, dust ingress, and a cheap cooling system. But often the cause of overheating is too much current applied to the board components. That is why it is extremely important to calculate such a current strength for each element in order to prevent breakage due to overheating in advance during the practical use of any board

II. MAIN RESULTS AND THEIR DISCUSSIONS

The PCB design process begins with creating a component library for the project. Automated placement of elements on the board should be carried out using the SolidWorks API [1]. The API application is developed directly in Visual Studio, using program code generated when writing a macro in SolidWorks.

To perform this work, the board is designed using the developed algorithm with several basic SMD components that were supplied with a current of 5A, resulting in heating of these components (fig. 1).

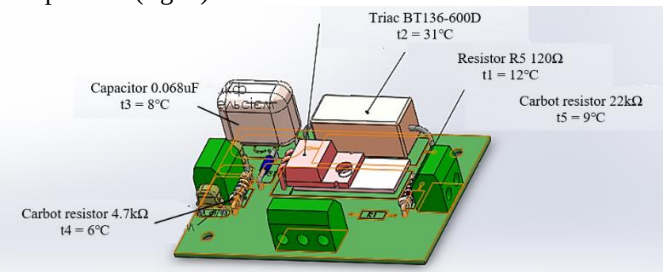

Fig. 1. Simulating the heating of board components in SolidWorks after applying a current of 5A

Heating in SolidWorks is conventionally represented by a gradient (blue – low heat, yellow/orange – low heat, red – high heat) using API mechanisms and functions.

As can be seen from the simulation, some elements were subjected to more heating than others due to individual technical characteristics and features. At this stage, we can already conclude that the TRIAC is heated most of all on the designed board (t = 31C), which is still within acceptable limits, but with a future increase in the current strength, you need to pay attention to this component.

After performing the simulation, the board was analyzed using Flow Simulation methods.

III. CONCLUSION

The developed automated subsystem helps simplify the placement of components that can be selected from the library on the printed circuit board. For proper placement of elements, the subsystem takes into account not only that the element does not extend beyond the board, but also its thermal characteristics. At the same time, printed circuit boards are used in almost every electronic device, but they are very vulnerable to overheating, which is a consequence of incorrect current supply to SMD components. Thanks to the analysis, you can determine exactly how much current the board elements can withstand, so as not to burn out due to too high a temperature during operation, and using Flow Simulation methods, you can better get acquainted with the results of the simulation.

REFERENCES

[1] Halushko Oleksandr, Kretovych Nazarii, Lizanets Danylo, Kolesnyk Kostyantyn. Application of the SW API for an Automatization of the Basic Elements of Design Cycle // Advanced technologies and methods of MEMS design: proceedings of the tenth international conference MEMSTECH 2014, June 22-24, 2014, Lviv, Ukraine / National university "Lviv polytechnic"- Lviv - Polyana: Publishing House Vezha&Co. 2014 - Pp.1-3.

[2] R. Panchak, K. Kolesnyk, M. Lobur. Topology Editing Strategies In The Subsystem Of Printed Circuit Boards Manufacturability Improvement. Proc. of the XI Intern. Conf. on The Experience of Designing and Application of CAD Systems in Microelectronics (CADSM'2011). - Lviv - Polyana: Publishing House Vezha&Co. 2011. - Pp. 246-247.

[3] R. Panchak, K. Kolesnyk. Subsystem of Technological Editing of Topology of Plated Circuits. Proc. of the VIth International Conference MEMSTECH'2010. - Lviv - Polyana: Publishing House Vezha&Co. 2010.- Pp. 121-122.

CONTROL SYSTEM FOR AN EXPERIMENTAL MODEL OF ROBOTIC MOBILE PLATFORM WITH MANIPULATOR

Vitaliy Mazur[1], Sofiia Panchak[2]
Lviv Polytechnic National University[1]
Vitaliy.V.Mazur@lpnu.ua
Lviv Polytechnic National University[2]
Sofiia Panchak@lpnu.ua

ABSTRACT

The control system for robotic mobile platform with manipulator is considered in the work. To ensure the required speed and accuracy of the platform positioning the method for changing the speed of the drive stepper motors is proposed. The method of collisions elimination at movement of several mobile platforms on the marked surface is offered.

KEYWORDS: **robotic mobile platform, experimental model, manipulator, control system, container transportation.**

I. INTRODUCTION

Robotic mobile platforms are increasingly used at automation of technological processes. To simplify the control system and traffic planning, an experimental model of a robotic mobile platform for moving on orthogonal routes was proposed in [1]. The kinematic scheme of the manipulator and ensuring the accuracy it positioning when containers moving are considered in [2].

This paper considers the problems of providing the movement of a platform with variable speed to increase the accuracy of positioning and ensuring the joint movement of several platforms.

II. STEPPER MOTOR SPEED CONTROL

Elimination of dynamic overloads and skipping steps (to ensure the required positioning accuracy) is based on a controlled smooth change of the stepper motor speed (Fig. 1).

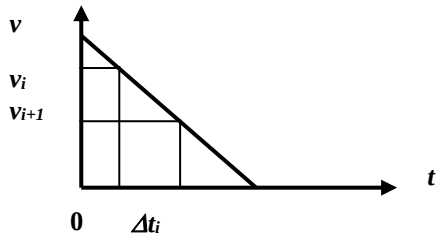

Fig. 1. Dependence of the speed on pulse duration

To determine the pulse duration Δt_i , which varies for each step of the motor during deceleration and acceleration, the following formulas are proposed:

$$v_{i+1} = v_i + a \times \Delta t_i \quad (1)$$

Where: a - set deceleration (-3 cm / sec^2); v_i - is the initial value of the platform speed (v_i = 3 cm / sec); v_{i+1} - the value of the platform speed after time Δt_i .

The distance s that the platform passes in one step of the motor is

$$s = (v_{i+1} + v_i) / 2 \times \Delta t_i = \pi \times d \times n / k \quad (2)$$

Where: d - is the diameter of the wheel; n - is the number of the gearbox shaft revolution per second; k - is the number of pulses per one revolution of the motor shaft.

Using relations (3) and (4), an array of values Δt_i (i = 1, 256) is determined, which is used by the controller to generate pulses.

$$\Delta t_i^2 + 2 \times v_i / a \times \Delta t_i - 2 \times s / a = 0 \quad (3)$$

$$\Delta t_i = (- v_i + ((v_i^2 + 2 \times s \times a)^{1/2}) / a \quad (4)$$

III. COLLISIONS ELIMINATION OF SEVERAL PLATFORM

To eliminate collisions during the movement of several platforms, the marked surface is divided into zones 21×21 cm (Fig. 2). When planning the movement, a matrix $M\ (i, j, m)$ is formed in which the beginning and end of the time of the platform m location in the zone (i, j) are fixed. Time diversity is provided by the introduction of additional delays based on analysis of the matrix.

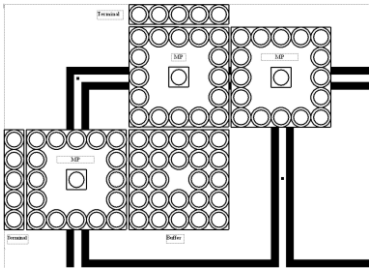

Fig. 2. Division of the marked surface into zones

REFERENCES

[1] V.V. Mazur and S.T. Panchak, “Experimental Model of a Mobile Platform for Moving on Orthogonal Routes”, CAD in Machinery Design: Implementation and Educational Issues (CADMD 2020), IOP Conf. Series: Materials Science and Engineering, 1016 (2021) 012011 DOI:10.1088/1757-899X/1016/1/ 012011.

[2] V.V. Mazur, “Robotic Mobile Platform for Container Transportation”, 2021 IEEE 16th International Conference on Experience of Designing and Application of CAD System (CADSM 2021), pp. 10-13, DOI:10.1109/CFDSM 52681.2021.985212.

CREATING MATERIALS WITH THE SPECIFIC ELECTROMAGNETIC PROPERTIES USING THE ASYMPTOTIC APPROACH

Mykhaylo Andriychuk
Lviv Polytechnic National University
Pidstryhach Institute for Applied Problems of Mechanics and Mathematics, NASU
mykhaylo.i.andriychuk@lpnu.ua, andr@iapmm.lviv.ua

ABSTRACT

The possibility to create the material with the specific electromagnetic (EM) parameters, including its permittivity, permeability and the refractive index are discussed in the paper. The procedure is based on the embedding a set of micro/nano particles into initial homogeneous material. The new inhomogeneous structure becomes different of the initial one the determinative material parameters. In order to obtain the explicit formula for the extracted parameters, the respective scattering problem is solved by series of asymptotic assumption about smallness of the embedded particles. The numerical simulation allows to obtain the permittivity and permeability of the resulting material, which differ in the great extent in comparison with the initial material parameters. The negative values of refractive index can be achieved in the framework of the approach proposed.

KEYWORDS: **EM scattering, asymptotic approach, specific material parameters, computational modeling.**

I. INTRODUCTION

The asymptotic approach is applied successfully for the analytical solving the electromagnetic (EM) wave scattering problems on a set of micro/nano bodies [1]. The excellence of this approach is its feasibility to get an approximate solution in the closed form that is a convenient condition to use it for many engineering applications.

The material with a placed set of small bodies gets a new physical property. Namely, it can be characterized by the permeability $\mu(x)$ with spatial inhomogeneity, and it can be changed either by the value of surface boundary impedance of particles or by their distribution density.

It turned out that even though the initial material has a permeability μ_0 that is constant, the obtained specimen has a non-homogeneous distribution of $\mu(x)$. This distribution can be derived in the closed form using either the characteristic density of the located particles or the boundary impedance of particles. This new physical phenomena was announced firstly in [2], and secondly it was supported by computations in [3] in the case of conformal particles.

II. THE NEW MATERIAL PARAMETERS OF RESULTING SPECIMEN

The solution to EM wave scattering problem on a set of large number M of small size particles can be written as

$$E(x) \approx E_0(x) + \sum_{m=1, m\neq j}^{M} [\nabla_x g(x, x_m), Q_m], \qquad (1)$$

where $E_0(x)$ is incident field, $g(x, x_m)$ is the Green function, Q_m is some additional function, which can be given in the terms of $E(x)$ that leads to possibility to obtain the respective linear algebraic system at the numerical implementation. By ∇_x is marked the derivative of $g(x, x_m)$ with the respective coordinate.

After the values of electric field $E(x)$ are determined, the new resulting permeability $\mu(x)$ is obtained as

$$\mu(x) = \frac{\mu_0}{1 + \frac{8\pi i}{3\omega\mu_0} h(x) N(x)}, \qquad (2)$$

and the refractive index n is determined using the explicit representation $n = \omega\sqrt{\varepsilon_r(x)\mu(x)}$ too. In the last formula, function $h(x)$ describes the surface impedance of particles, and function $N(x)$ determines the quantity of the embedded particles. The new permittivity $\varepsilon(x) = \varepsilon_0\varepsilon_r(x)$, where ε_0 is permittivity of the initial material.

The computational data are in the concordance with the physical sense, namely the values of $\mu(x)$ and n tend to the parameters of the initial medium, when the characteristic size of particles decreases or the distance between them increases.

III. CONCLUSION

The derived closed form asymptotic solution of EM wave scattering problem on a set of small particles allowed to obtain the explicit formulas for the material parameters of the inhomogeneous specimen, including its permittivity, permeability, as well as the refractive index including its negative values.

REFERENCES

[1] A. G. Ramm, Scattering of acoustic and electromagnetic waves by small impedance bodies of arbitrary shape. Application to creating new engineering materials. New York: Momentum Press, 2013.

[2] A. G. Ramm, "Wave scattering by many small particles embedded in a medium," Phys. Lett. A, vol. 372, no. 17, pp. 3064–3070, 2008.

[3] A. G. Ramm, M. I. Andriychuk, "Application of the asymptotic solution to EM field scattering problem for creation of media with prescribed permeability," J. Appl. Math. Comput., vol. 45, no. 1, pp. 461–485, 2014, doi: 10.1007/s12190-013-0732-7.

DEVELOPMENT OF METHODS FOR DETECTING NETWORK ATTACKS ON CYBER-PHYSICAL SYSTEMS

Olexander Belej , Iryna Artyshchuk, Nataliia Spas, Natalia Nestor
Oleksandr.I.Belei@lpnu.ua., iryna.v.artyshchuk@lpnu.ua., nataliia.y.spas@lpnu.ua., natalia.nestor@gmail.com
Lviv Polytechnic National University

ABSTRACT

In the presented research the technique of application of neuroevolutionary algorithms in processes of detection of network attacks on cyber-physical systems is offered. During the implementation of this technique, the accuracy of the developed system for detecting network attacks was evaluated. The principle of operation of such a system is to identify deviations between the current values of the state of cyber-physical systems and the predicted results. The forecast is based on the neuroevolutionary algorithm of the NeuroEvolution of Augmenting Topologies family.

KEYWORDS: **cyber-physical systems, neuroevolutionary algorithm, detection of network attacks, application, operation.**

I. INTRODUCTION

After a thorough analysis of existing methods of data representation in cyber-physical systems (CPS) [1]. Direct creation and implementation of your method for detecting network attacks on CPS [2].

The described method will be based on processing the obtained time series from actuators and CPS sensors, using the modified NEAT-hypercube algorithm to predict the subsequent state of the system, and calculating the error between the predicted and real values.

Testing of the created and implemented method for detecting network attacks on CPS will be performed on the TON_IOT DATASETS dataset [3].

II. RESULTS

Fig. 1 and Fig. 2 show results of displaying normalized data about the state of the system during 48 hours of its operation in a normal state and in a state that includes abnormal behavior.

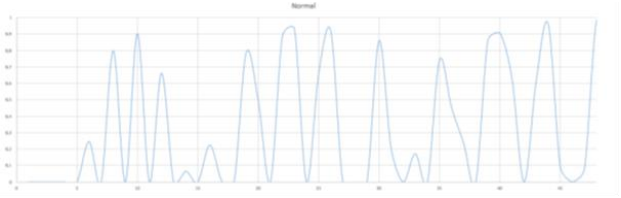

Fig. 1. Data changes within 48 hours of normal system operation

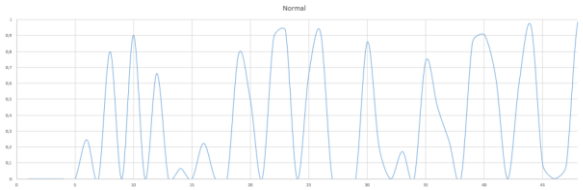

Fig. 2. Data changes within 48 hours of working with DDoS attacks

The working stage implies the direct detection of network attacks directed at the CPS and includes the following steps: preparation of real data of the functioning CPS - normalization, and compilation of multidimensional time series; transmission of the obtained multidimensional series to the input of the neural network, the optimally configured genetic component of the neuroevolutionary algorithm; prediction of the future state of the system by a neural network based on the obtained multidimensional time series; calculating the error between the predicted state of the system and the real one; fixing the presence or absence of attacks on the CPS based on the received error (Fig. 3).

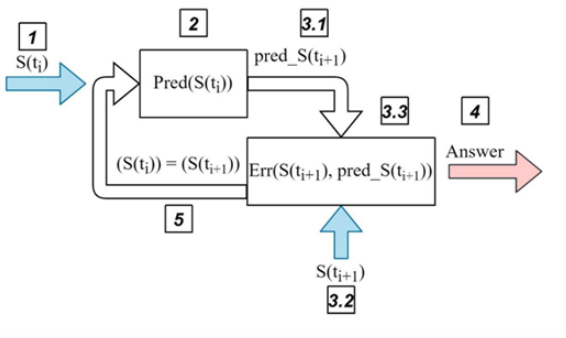

Fig. 3. Schematic diagram of the operation of the method for detecting network attacks

III. CONCLUSIONS

The result of this work is the creation, implementation, and experimental research of the implemented method for detecting network attacks carried out on the CPS. The method includes the use of a neuroevolutionary algorithm of the NEAT family: modified NEAT-hypercube.

REFERENCES

[1] Kim, S.; Park, K.-J. A Survey on Machine-Learning Based Security Design for Cyber-Physical Systems. Appl. Sci. 2021, 11, 5458.
[2] C. A. R. de Sousa, "An overview on weight initialization methods for feedforward neural networks," 2016 International Joint Conference on Neural Networks (IJCNN), 2016, pp. 52-59.
[3] TON_IOT_DATASETS. – URL: https://ieee-dataport.org/documents/toniot-datasets.

DEVELOPMENT OF ALGORITHMIZATION BASES FOR JET TREATMENT EVALUATION MODES OF PRODUCT CURVILINEAR SURFACES

Zinoviy Stotsko[1], Tetyana Stefanovych[2]
Lviv Polytechnic National University[1]
stotsko@lp.edu.ua
Lviv Polytechnic National University[2]
tetyana.o.stefanovych@lpnu.ua.

ABSTRACT

Method and algorithm for evaluating the angular and linear velocities of the jet nozzle or product are proposed to ensure uniform jet treatment for curvilinear surfaces of products.

KEYWORDS: **jet treatment, technological equipment, mechanical movement, process modes, curvilinear surface.**

I. INTRODUCTION

For products of complex shape, jet treatment is often an unalterable method of ensuring the desired surface quality. It is possible to provide the desired results of jet treating if the process modes are set correctly. Therefore, it is reasonable mathematical modeling for various processing cases, especially at the processing of difficult-profile surfaces. Its results will be useful when designing process equipment.

II. LITERATURE REVIEW

Many studies are associated with the experimental searching of process modes for different material brands [1, 2]. Theoretical research is based on the energy concept [3, 4]. It is used to evaluate the mass distributions of the flow medium along a flat fixed surface or the radius of the rotating faceplate surface [5].

III. PROCESS CONDITIONS AND MODES

It is necessary to ensure such conditions for the uniform treatment of curvilinear surfaces:

1. a constant distance from the nozzle end to the treated surface L;

2. the perpendicularity of the jet apparatus nozzle axis to the curvilinear surface generatrix.

The following process modes should be provided for ensuring this:

1. the workpiece must be in translational motion, which can be described by equations:

$$x = x_a + V_x t \,, \quad y = y_a + V_y t \tag{1}$$

2. the linear velocities of the product or the jet apparatus nozzle must correspond to the ratio:

$$V_y = V_x \frac{df(x)}{dx} \tag{2}$$

3. the angular velocity of the nozzle should be:

$$\omega = \frac{d(\operatorname{arctg}\frac{df(x,t)}{dx})}{dt} \tag{3}$$

According to (1)-(3) the dependences of the process modes on time for further algorithmization of the nozzle movement modes and the product are obtained and designing the drive devices of the technological equipment (Fig. 1).

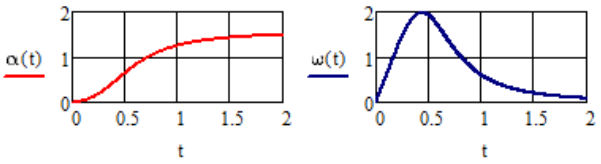

Fig. 1. The angle of tangent inclination $\alpha(t)$ to the surface given by the cubic parabola $y(t) = t^3$, and the nozzle angular velocity for $L = 1$, $V_x = 1$

IV. CONCLUSIONS

The method and algorithm for evaluating jet treatment velocity are offered, and graphs of linear and angular speeds over processing time of complex profile surfaces are received.

REFERENCES

[1] W. S. Slat, V. Malau and P. T. Iswanto, "The Effects of Shot Peening Treatment on the Hardness and Fatigue Strength of HQ 805," 2018 International Conference on Applied Science and Technology (iCAST), 2018, pp. 142-145, doi: 10.1109/iCAST1.2018.8751516.

[2] X. Li and C. Jiang, "Numerical Simulation Analysis of Shot Peening Residual Stress on Aluminum Alloy Surface Based on Finite Element Method," 2019 6th International Conference on Dependable Systems and Their Applications (DSA), pp. 183-190, 2020, doi: 10.1109/DSA.2019.00030.

[3] Stotsko Z.A., Stefanovych T.O., "Investigations on the Machine Parts Treatment by Non-bound Blast Particles, Journal of Achievements in Materials and Manufacturing Engineering," vol. 49, no 2, pp. 440-459, 2011, , url: http://jamme.acmsse.h2.pl/papers_vol49_2/49236.pdf.

[4] N. Liu et al., "Modelling of abrasive blasting process from viewpoint of energy exchange," 2018 IEEE 23rd International Conference on Emerging Technologies and Factory Automation (ETFA), 2018, pp. 488-492, doi: 10.1109/ETFA.2018.8502548.

[5] Stotsko Z.A., Stefanovych T.O., "Surface Layer Modelling and Diagnostic after Loose Solid Balls Treatment", Przetwórstwo Tworzyw", vol. 17, no 6 (144), pp. 529-533, 2011, url: https://yadda.icm.edu.pl/yadda/element/bwmeta1.element.baztech-article-BPC5-0007-0024.

DEVELOPMENT OF MICROCONTROLLER BASED TEMPERATURE AND HUMIDITY DATA LOGGER

Andriy Holovatyy, Roman Panchak, Mykhaylo Lobur
Department of Computer-Aided Design Systems, Lviv Polytechnic National University
andrii.i.holovatyi@lpnu.ua, roman.t.panchak@lpnu.ua

ABSTRACT

In the paper, the hardware and software of the microcontroller based temperature and humidity data logger has been developed. The device measures temperature and humidity, displays the temperature and humidity values on the LCD and writes them to the file in CSV format on the microSD memory card. The operation algorithm of the microcontroller temperature and humidity data logger has been developed. The software modules for communication with the digital temperature and humidity sensor HTU21D, outputting information to the alphanumeric LCD module HD44780 and data processing software have been created. The model of the microcontroller based temperature and humidity data logger in Proteus ISIS has been created and simulated. The prototype of the microcontroller based temperature and humidity data logger has been created and tested.

KEYWORDS: **microcontroller temperature and humidity data logger, HTU21D, RobotDyn shield micro SD card reader + RTC DS1307, alphanumeric LCD HD44780, ATmega328P-PU, Proteus VSM, embedded software, Arduino IDE.**

I. INTRODUCTION

The current state of development of electronics makes it possible to create cheap measuring systems based on microcontrollers and various sensors. In particular, it can be a microcontroller temperature and humidity data logger.

The temperature and humidity data loggers are compact, stand-alone devices that record ambient temperature and humidity values for a specified time at specified intervals, store them, and transmit this data to external devices in a specified format. The temperature and humidity data loggers are widely used in production and other activities in which there are increased requirements for the quality of environmental parameters [1].

II. DEVELOPMENT OF MICROCONTROLLER BASED TEMPERATURE AND HUMIDITY DATA LOGGER

In Fig. 1 the block diagram of the microcontroller data logger is shown. The data logger hardware consists of the Arduino Uno R3 board [2-4], digital temperature and humidity sensor HTU21D [5], RobotDyn module (RTC IC DS1307 and microSD card reader) [6, 7], 4 keys keypad and alphanumeric 16×2 LCD HD44780 [7]. The Arduino Uno reads data from the HTU21D sensor, processes and writes them to the memory card in real time. The current temperature and humidity values, date and time are also displayed on the alphanumeric LCD.

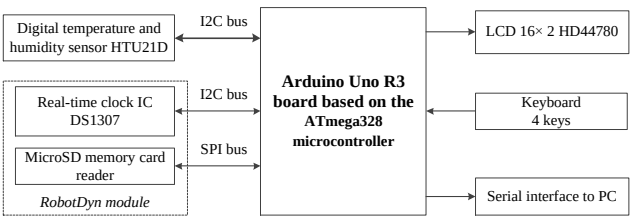

Fig. 1. Block diagram of the data logger

In Fig. 2, the hardware of the data logger in CAD Proteus is shown.In the circuit, the temperature and humidity sensor HTU21D is connected to the Arduino Uno board using the I2C bus. The SCK and SDA sensor lines are connected to the A4 (SDA) and A5 (SCL) pins of the I2C bus of the Arduino Uno. The RTC IC DS1307 is also connected to the I2C bus of the Arduino Uno board. The SCL and SDA lines of the I2C bus on the Arduino Uno board are located on the pins 19 (A5/SCL) and 18 (A4/SDA). The microSD card reader is connected to the Arduino Uno card via the SPI interface. The SCK pin of the card reader is connected to the pin 13, the MISO pin to the pin 12, the MOSI pin to the pin 11, and the CS pin to the pin 9 of the Arduino Uno board. The LCD is connected to the pins of the PBx and PDx ports. The MENU_BTN button is connected to the pin 2, the SEL_PLUS_BTN button to pin 17, the SEL_MINUS_BTN button to the pin 16 and the EXIT_BTN to the pin 3 of the Arduino Uno board.

III SIMULATION AND PROTOTYPE TESTING OF MICROCONTROLLER BASED TEMPERATURE AND HUMIDITY DATA LOGGER

The data logger software is written using Arduino IDE [7]. Before downloading the firmware to the device, its operation can be checked on the created model in Proteus ISIS, Fig. 2.

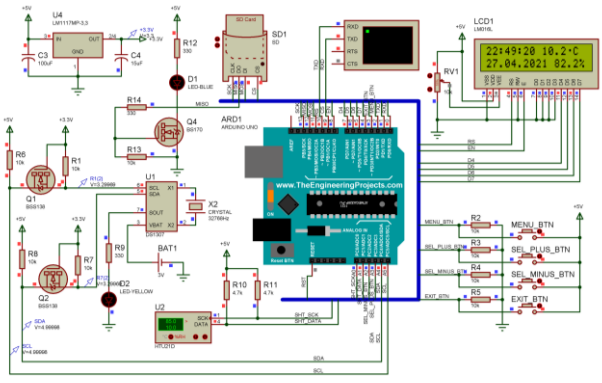

Fig. 2. Simulation of the data logger in Proteus ISIS

In Fig. 3 - 4 the testing of the prototype of the temperature and humidity data logger is shown.

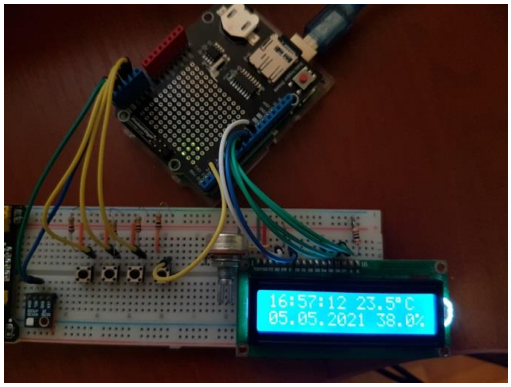

Fig. 3 Prototype of the microcontroller based temperature and humidity data logger

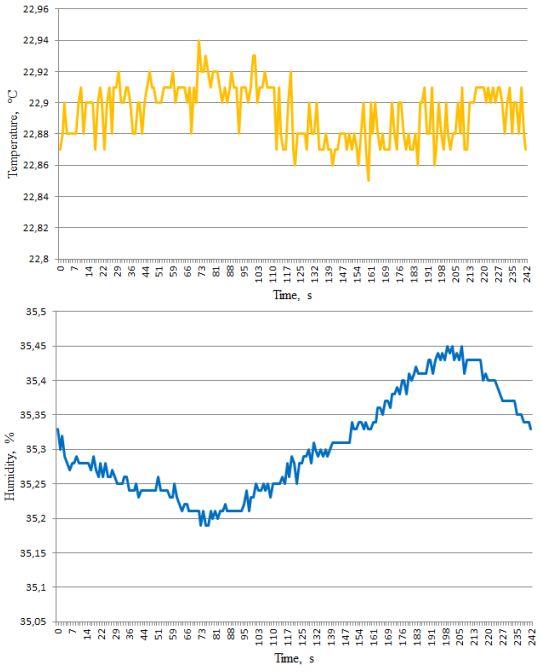

Fig. 4 Excel graphs of temperature and humidity data written by using the developed data logger

IV. CONCLUSIONS

In the work, the hardware and software of the microcontroller temperature and humidity data logger are developed. The device measures temperature and humidity, displays the measured temperature and humidity values on the alphanumeric 16x2 LCD HD44780 and writes them in a .csv file to the microSD memory card. The electronic circuit of the microcontroller temperature and humidity data logger in the Proteus CAD system has been designed. The operation algorithm and data processing software of the microcontroller based temperature and humidity data logger has been developed. The software modules for communication with the digital temperature and humidity sensor HTU21D, for outputting information to the alphanumeric LCD module HD44780 have been created. The model of the microcontroller based temperature and humidity data logger in Proteus ISIS has been created and tested.

The prototype of the microcontroller based temperature and humidity data logger has been developed and tested.

REFERENCES

[1] Electronic resource on data loggers: https://www.testo.com/en-IN/products/datalogger-humidity, https://www.testo.com/en-IN/products/-datalogger humidity

[2] Massimo Banzi. Getting Started with Arduino. 2nd Edition. O'Really Media Inc., 2011 p. 130.

[3] Electronic resource on HTU21D: https://cdn-shop.adafruit.com/datasheets/1899_HTU21D.pdf.

[4] Electronic resource on RTC DS1307: https://pdf1.-alldatasheet.com/datasheet-pdf/view/123888/-DALLAS/DS1307.html, https://datasheets.maxim-integrated.com/en/ds/DS1307.pdf.

[5] Electronic resource on the RTC+microSD card shield from RobotDyn: https://arduino.ua/prod2645-shild-rtcsd-card dlya arduino uno ot robotdyn.

[6] Electronic resource on LCD HD44780 controller/driver: https://www.sparkfun.com/datasheets/LCD/HD44780.pdf

[7] Electronic resource on Arduino IDE: https://www.arduino.cc/en/Main/Software.

ENGINEERING DRAWING EDUCATION USING CAD TOOLS

Andrzej Łukaszewicz[1], Andriy Kernytskyy[2], Mykhaylo Melnyk[2]
Bialystok University of Technology [1]
Lviv Polytechnic National University [2]
a.lukaszewicz@pb.edu.pl
kernitsky@gmail.com
melnykmr@gmail.com

ABSTRACT

The paper presents selected aspects of engineering drawing education used in Faculty of Mechanical Engineering, Bialystok University of Technology and Department of Computer Aided Systems, Lviv Polytechnic National University. Nowadays this is inextricably linked with CAD and CAx techniques. Some issues of engineering drawing and CAD education are outlined based of the authors' many years of experience in teaching of the mechanical engineering drawing, MCAD, ECAD and MEMS.

KEYWORDS: **CAD education, engineering drawing, mechanical engineering.**

I. INTRODUCTION

Engineering drawing is essential subject in engineering education [1, 2]. Technical drawing - made in accordance with regulations and applicable rules - is the language used by engineers and technicians of all countries to communicate. The universal and international importance of technical drawing enables inventions and improvements from around the world. Technical drawing is a form of idealization and simplification of the actual features of the depicted objects in order to facilitate their description. Technical drawing is a graphical representation that conventionally forwards accurate information about the shape, dimensions, and performance characteristics of individual parts, assemblies, and whole devices.

The long experience of the authors in technical universities teaching process, supported by many papers [3-20], provides an opportunity for historical analysis and forecasting of further method of technical drawing, CAD and CAx systems teaching in both mechanical and electro-mechanical field (eg. MEMS).

REFERENCES

[1] Bajkowski J. (2011) Podstawy zapisu konstrukcji. Warszawa, Oficyna Wydawnicza Politechniki Warszawskiej,
[2] Bajkowski J., Bajkowski J.M. (2019) Podstawy zapisu konstrukcji. Materiały do ćwiczeń projektowych. Zadania z rozwiązaniami. Warszawa, Wydawnictwo Naukowe PWN,
[3] Łukaszewicz A. (2006): „Rola i rozwój współczesnych systemów CAD", V Konferencja naukowo – praktyczna „Energia w Nauce i Technice" Suwałki, pp. 95-98,
[4] Łukaszewicz A. (2008): „CAx education as an inseparable part of integrated product development", In: "Design methods for industrial practice" (ed. R. Rochatyński), Oficyna Wydawnicza Uniwersytetu Zielonogórskiego, pp. 313-320,
[5] Łukaszewicz A. (2008): „Selected aspects of parametric CAD systems education", XVI Ukrainian-Polish Conference on CAD in Machinery Design. Implementation and Educational Problems: CADMD'2008; pp. 42-44,
[6] Łukaszewicz A. (2009): „General advices to the CAx education directed for needs of the industry", In: „Advanced technologies in production engineering" (ed. J. Józwik), Societas Scientiarum Lublinensis, Lublin 2009, pp. 73-86,
[7] Łukaszewicz A. (2009): "Selected problems of CAD education directed for industrial practice", Scientific Gerald of Lviv Polytechnic National University, No. 651, pp. 225-231,
[8] Łukaszewicz A. (2009): „General rules of parts and assemblies modelling in parametric CAD systems", Machine Dynamics Problems, Vol. 33, No 3, pp. 49-55,
[9] Łukaszewicz A. (2010): „Zagadnienia wdrażania parametrycznych systemów CAx w sektorze przemysłowym branży mechanicznej", Mechanik, nr 1/2010, pp. 142-146,
[10] Łukaszewicz A. (2010): „SolidWorks based CAx Education Directed for Industrial Practice ", SolidWorks World 2010, Anaheim, USA, 23,
[11] Łukaszewicz A. (2011): „Sources of innovative UAV design", XIX Polish-Ukrainian Conference on CAD in Machinery Design. Implementation and Educational Problems: CADMD'2011, pp. 27-28,
[12] Łukaszewicz A., Kernytskyy A. (2011): „Rapid prototyping in UAV applications on the example of 3D printing technique", XIX Polish-Ukrainian Conference on CAD in Machinery Design. Implementation and Educational Problems: CADMD'2011, pp. 29-30,
[13] Łukaszewicz A., Kernytskyy A. (2012): „ CAx System as an Education Platform in Mechanical Branch", XX Ukrainian-Polish Conference on CAD in Machinery Design. Implementation and Educational Problems: CADMD'2012, pp. 31-33,
[14] Jabłoński M., Łukaszewicz A. (2013): "Approaches to assemblies modelling in MCAD systems", XXI Polish-Ukrainian Conference on CAD in Machinery Design. Implementation and Educational Problems: CADMD'2013, pp. 15-16,
[15] Panas K., Łukaszewicz A. (2013): "Effective work in design of new product in MCAD systems", XXI Polish-Ukrainian Conference on CAD in Machinery Design. Implementation and Educational Problems: CADMD'2013, pp. 43-44,
[16] Jabłoński M., Panas K., Łukaszewicz A. (2013): „Koncepcyjne projekty urządzeń wykonane przy użyciu oprogramowania 3D CAD", W: Komputerowe wspomaganie nauki i techniki CAX, T. 1, (red. T. Mikołajczyk) , pp. 43-52,
[17] Łukaszewicz A. (2014): "Approach to understanding of design process at parametric, history-based CAD systems", XXII Polish-Ukrainian Conference "CAD in Machinery Design - Implementation and Educational Issues" CADMD 2014, pp. 186-187,
[18] Łukaszewicz A., Panas K., Szczebiot R. (2018): "Design process of technological line to vegetables packaging using CAx tools". Proceedings of 17th International Scientific Conference on Engineering for Rural Development, May 23-25, 2018, Jelgava, Latvia, pp. 871-876,
[19] Łukaszewicz A., Skorulski G., Szczebiot R. (2018): "The main aspects of training in the field of computer-aided techniques (CAx) in mechanical engineering", Proceedings of 17th International Scientific Conference on Engineering for Rural Development, May 23-25, 2018, Jelgava, Latvia, pp. 865-870,
[20] Łukaszewicz A, Trochimczuk R, Melnyk M, Kernytskyy A. (2021): "Design of mechatronics systems using CAx environment", In: (Butryło B, ed.) Methods and Tools in CAD – Selected Issues, Oficyna Wydawnicza Politechniki Białostockiej, pp. 7-14,

INVESTIGATION OF SOUND LEVEL METERS ACCURACY IN DETERMINING THE EQUIVALENT SOUND LEVEL

Mykhaylo Melnyk[1], Andriy Kernytskyy[1], Andrzej Lukaszewicz[2], Mykhailo Lobur[1], Andriy Zdobytskyi[1], Krzysztof Pytel[3]
Lviv Polytechnic National University[1]
melnykmr@gmail.com, Andriy.B.Kernytskyy@lpnu.ua, andrii.y.zdobytskyi@lpnu.ua
Bialystok University of Technology [2]
a.lukaszewicz@pb.edu.pl
AGH University of Science and Technology[3]
kpytel@agh.edu.pl

ABSTRACT

The paper describes the results of experimental determination of the equivalent sound level of sound noise meters of different accuracy class. Software has been developed to determine the equivalent sound level based on sound pressure levels recorded by a sound level meter. A comparative analysis of the obtained results was performed.

KEYWORDS: **sound noise meters, SL5868BT, MATLAB, SVAN958A, equivalent noise level, acoustic measurements.**

I. INTRODUCTION

Expensive integrating sound level metershave to be used to measure the equivalent sound level, which is regulated by state building codes, state sanitary norms and state standards, as cheap analogues do not have the ability to determine the equivalent noise level. In this regard, the task is to study the possibility of integrating data from low-cost sound level meters with a computer to determine equivalent sound level based on sound pressure levels.

Software in the MATLAB system [2] has been developed to calculate the equivalent sound level based on the sound pressure levels obtained from the SL5868BT [1]. The SVAN 958 accuracy class 1 sound level meter was used as a reference [3]. The omnidirectional sound source was used as a test source of white noise [4]. The process of conducting acoustic research (see Fig. 1) was to compare the equivalent sound levels obtained from an inexpensive sound level meter, calculated in the developed system and obtained from the reference device. The result of comparing different methods for determining the equivalent noise level is presented in Fig. 2

Fig. 1. Conducting an experiment

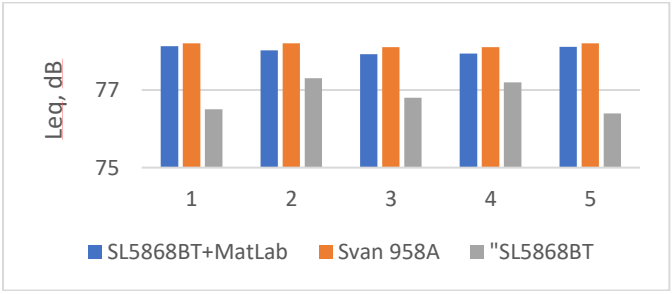

Fig. 2. Results

It can be seen from the diagram in Fig. 2 that the errors between the reference device and the results obtained using the equivalent software to calculate the equivalent noise level are small. On the other hand, the discrepancy between the reference values and those obtained directly from an inexpensive sound level meter is much larger.

CONCLUSIONS

As a result of the conducted research it was established that the hardware of the inexpensive sound level meters for carrying out integration of sound pressure levels in order to determine the equivalent sound pressure level is inaccurate. Increased accuracy can be achieved by performing an integration operation on a computer.

REFERENCES

[1] 1. Sound Level Meter SL-5868P [Electronic resource]. – 2020. – Mode of access to the resource: http://www.landtek.com.cn/en/pd.jsp?id=1957

[2] SVAN 958 Four Channels Sound & Vibration Analyser [Electronic resource]. – 2020. – Mode of access to the resource: https://svantek.com/pub/files/File/produkty/datasheet/SVAN958.pdf

[3] Bradley, Samuel D. "Matlab." The International Encyclopedia of Communication Research Methods (2017): 1-3.

[4] Melnyk, M., Vynarovych, R., Kvasnytsya, T., & Lobur, M. (2018, February). Designing of omnidirectional speaker for automation of acoustic measurement process. In 2018 14th International Conference on Advanced Trends in Radioelecrtronics, Telecommunications and Computer Engineering (TCSET) (pp. 380-383). IEEE.

NUMERICAL ANALYSIS OF COLD EXTRUSION OF TUBES USING CAX SYSTEM

Grzegorz Skorulski[1], Andrzej Łukaszewicz[1]
Bialystok University of Technology [1]
g.skorulski@pb.edu.pl
a.lukaszewicz@pb.edu.pl

ABSTRACT

The paper presents a solution of pressure distribution problem in cold extrusion of tubes using finite element method (FEM), along with a procedure for preparing a computer simulation. In particular, the influence of the friction coefficient between die and workpiece has been analyzed. As a results, using CAD/CAE system, the diagrams of pressure distribution for each node in the CAD model of the die in several time steps have been obtained and presented. Additionally some aspect of quality of final solution has been discussed.

KEYWORDS: **cold extrusion, tubes, friction, contact stresses distribution.**

I. INTRODUCTION

CAx (CAD/CAM/CAE) tools are widely used in engineering fields [1, 2]. The main advantage of using CAx systems is a shortening of the product's time development. The ability to perform many types of CAE analyses [3, 4], visualization and technical documentation in the design phase allows you to better fit the assumptions.

Cold extrusion is defined as a compressive forming process (push-through), in which the source material is billet (slug), and the process is carried out at the room temperature. Deformation heating is the process of conversion of deformation work to heat. As a rule, a punch is used for applying pressure to the enclosed billet in the stationary die. With regard to the punch and the die design along with the resulting material flow, we can classify cold extrusion into three major categories: forward, backward and lateral extrusion. The basics of cold extrusion processes are described in [5, 7].

The design and manufacture of dies and the selection of die materials are very important in the production of discrete parts by means of metal-forming processes. The dies must be obtained by modern manufacturing methods from appropriate die materials, ensuring acceptable die life at a reasonable cost [6]. For a given application, selection of the appropriate die material depends on three types of variables:
a) variables related to the process itself, including factors such as size of the die cavity, type of machine used and deformation speed, initial stock size and temperature, die temperature to be used, lubrication, production rate and number of parts to be produced.

b) variables related to the type of die loading, including speed of loading, contact time (impact or gradual contact) between dies and deforming metal; the contact time is particularly important in hot forming, maximum load and pressure on the dies, maximum and minimum die temperatures, number of loading cycles to which the dies will be subjected.

c) mechanical properties of the die material, including hardenability, impact strength, hot strength (if hot forming is considered) and resistance to thermal and mechanical fatigue.

In the present work a tube extrusion process has been scrutinized. In particular, a solution of the pressure problem by means of a computer simulation using PAM - STAMP system [11] in the above process has been proposed. Also, a method of obtaining the contact stresses distribution during extrusion has been shown. Since the contact stress distribution is still relatively unknown and complex problem, the obtained results are of relevance to the field. The detailed knowledge about the process will help to streamline the die production processes.

II. PROBLEM STATEMENT

The pressure required to extrude a given section depends on:

a) flow stress $\overline{\sigma}$ of the extruded material under the existing temperature and extrusion conditions.
b) friction at the material/tool (container/die) interface [12, 13, 14],
c) reduction in area (cross-sectional area of billet/cross-sectional area of extruded section),
d) shape of extruded section.

The reduction in area and the section shape are given geometric variables. The frictional shear stress τ is defined as:

$$\tau = \frac{m \cdot \overline{\sigma}}{\sqrt{3}} \tag{1}$$

The friction factor m in non-lubricated hot extrusion has a fixed value m = 1. In lubricated hot extrusion $0.1 \leq m \leq 0.4$, with an estimated average m value of about 0.25 [9].

The flow stress is a function of temperature, strain, strain rate and structure. It is, therefore, determined by billet material, billet preheat temperature, container and die temperatures, extrusion ratio and extrusion speed. Due to temperature and strain-rate variations, the flow stress within the extruded material changes during the extrusion process. Consequently, in the practical estimation of extrusion pressure, it is sufficient to use an average value of flow stress, which is assumed to be valid for the whole deforming material. Thus, the calculated flow stress value can be used for estimating the extrusion pressures for other extrusion ratios and shapes [8, 10].

A review of theoretical methods and experimental studies reveals that the extrusion pressure p at the end of the extrusion stroke (i.e. without container

friction) [15] is a nearly linear function of the homogeneous extrusion strain, or:

$$p = a\ln(A_B/A_S) + b \quad (2)$$

where:
p - the extrusion pressure,
A_B - cross sectional area of the billet,
A_S - cross sectional area of the extruded section,
b - empirical constant which depends on material, press speed, temperature and section geometry.

During cold extrusion, material at different locations in the deformation zone is undergoes deformation to different extent. The value of strain $\overline{\varepsilon}$ and the corresponding flow stress $\overline{\sigma}$ vary within the deformation zone. It is necessary to use average values of the flow stresses $\overline{\sigma}$ and effective strain $\overline{\varepsilon}$ to characterize the total deformation of the material. Total forging load consist of the following components [16]:

$$P = P_{fd} + P_{fc} + P_{dh} + P_{ds} \quad (3)$$

where:
P_{fd} - load necessary to overcome friction at the die surface (in forward extrusion),
P_{fc} - load necessary to overcome container friction in forward extrusion,
P_{dh} - load necessary for ensuring homogeneous deformation,
P_{ds} - load necessary for internal shearing due to inhomogeneous deformation.

III. Conclusions

The loads are influenced by the following process variables [6, 16]:

- Extrusion Ratio R - the extrusion load increases with increasing reduction because the degree of deformation, i.e. the average strain $\overline{\varepsilon}_a$ increases with reduction.
- Die Geometry - the die geometry directly influences material flow, and therefore it affects the distribution of the effective strain and flow stress in the deformation zone. In forward extrusion, for a given reduction, a larger die angle increases the volume of material undergoing shear deformation and results in an increase of shear deformation load P_{ds}. On the other hand, the length of the die decreases, which results in a decrease of the friction load P_{fd}. Consequently, for a given reduction and in defined friction conditions there is an optimum die angle which minimizes the extrusion load.
- Extrusion Velocity - with the increasing velocity, both the strain rate and the temperature generated in the deforming material rise. These effects counteract each other, and consequently the load in cold extrusion is not significantly affected by the extrusion velocity.
- Lubrication - improved lubrication lowers the container friction force P_{fc} and the die friction force P_{fd} in equation (3), resulting in lower extrusion loads.
- Workpiece Material - the flow stress of the billet material directly influences the loads P_{dh} and P_{ds} in equation (3). The prior heat treatment or, as a matter of fact, any prior work hardening also affect the flow stress of the material. Therefore, flow stress values depend not only on the chemical composition of the material, but also on its prior processing history. As well as that, the temperature of the workpiece material influences the flow stress.
- Billet Dimensions - in forward extrusion, an increase in billet length results in an increase in container friction load P_{fc}.

In the present work, only the influence of friction coefficient between die/workpiece surface has been demonstrated.

References

[1] Łukaszewicz A., Skorulski G., Szczebiot R. (2018): "The main aspects of training in the field of computer-aided techniques (CAx) in mechanical engineering", Proceedings of 17th International Scientific Conference on Engineering for Rural Development, May 23-25, 2018, Jelgava, Latvia, pp. 865-870,

[2] Łukaszewicz A, Trochimczuk R, Melnyk M, Kernytskyy A. (2021): "Design of mechatronics systems using CAx environment", In: (Butryło B, ed.) Methods and Tools in CAD – Selected Issues, pp. 7-14,

[3] Sidun P, Łukaszewicz A. (2017): "Verification of ram-press pipe bending process using elasto-plastic FEM model", Acta Mechanica et Automatica, Vol. 11, Issue 1, 2017, pp. 47-52,

[4] Mircheski I., Łukaszewicz A., Szczebiot R. (2019): "Injection process design for manufacturing of bicycle plastic bottle holder using CAx tools", Procedia Manufacturing, Vol. 32, pp. 68-73,

[5] Luigino Filice, F. Gagliardi, F. Micari (2008), "A Laboratory Scale Equipment to Relieve Force and Pressure in Cold Extrusion of Lead Hollow Components", Key Engineering Materials, Vol. 367, pp. 137 - 144,

[6] Dieter E. G., Kuhn H. A., Semiatin S. L. (2003), "Handbook of workability and process design", ASM International,

[7] Stepanenko A. V., Isaevich L. A., Veremeichik A. A., Medvedeva T. A. (1987) "Theoretical investigation of the process of cold extrusion of rods from unplasticized metal powders. III. Extrusion pressure", Powder Metallurgy and Metal Ceramics, Volume 26, No. 7, pp. 519-523,

[8] Abou-El-Lail Mohsen M.M., Farag Mahmound M. (1981) "Analysis of direct extrusion by the finite element technique", Curr. Adv. Mech. Des. and Prod. Proc., 1st International Conference, Cairo 27 - 29 Dec. 1979, Oxford e.a. pp. 239 – 246,

[9] Webster W. D., Davis R.L. (1982) "Development of a friction element for metal forming analysis", Trans. ASME J. Eng. Ind, 104, No.3, pp. 253 – 256,

[10] Bhattacharyya S. , Mujamdar A. K., Basu S. K. (1982) "Mathematical modelling of metal extrusion process", Trans. ASME J. Eng. Ind, 104, No.1, pp. 65 – 70,

[11] PAM - STAMP User's Guide, (1997) ESI Group Software Product Company, France,

[12] Hrycaj P., Cescotto S., Oudin J. (1991) "Elasto - plastic finite element analysis of unilateral contact with generalised Coulomb friction", Engineering Computation, vol. 8, pp. 291 -303.

[13] Oden J. T., Pires E. B. (1983) "Numerical analysis of certain contact problems in elasticity with non-classical friction laws", Computers & Structures, vol.16, No. 1-4, pp. 481-485,

[14] Nine H. D. (1982) "The applicability of Coulomb's friction law to drawbeads in sheet metal forming", American Society of Metals, vol.2, No.3,

[15] Samper V., Felder E. (1990) "Frictional mechanism in uncoated and zinc-coated steel sheet forming - theoretical and experimental results", Mechanics and Coatings, Tribology series 17, Elsevier Science Publishers B.V.,

[16] Altan T., Ngaile G., Shen G. (2004) "Cold and Hot Forging. Fundamentals and Applications" ASM International,

NUMERICAL TESTS OF THE POWER COEFFICIENT THE VAWT WITH ODGV

Radosław Ptak, Krzysztof Kołodziejczyk
AGH University of Science and Technology
rptak@extremecnc.pl
AGH University of Science and Technology
krkooodz@agh.edu.pl

ABSTRACT

Currently, obtaining energy from renewable sources has become one of the most important areas, but at the same time challenges in human activity. This is the result of many factors at the same time, incl. due to the greenhouse effect publicized in the media, the need to reduce CO^2 emissions, the shrinking of natural resources, and thus the desire to protect them, including maintaining the welfare (including natural resources) for future generations. The article contains a numerical analysis of the operation of a wind turbine with a vertical axis of rotation with guide vanes. The conducted analyzes indicate the potential possibility of using this type of structure in practice.

KEYWORDS: **vertical axis wind turbine, numerical modeling.**

I. INTRODUCTION

The construction, of a vertical axis windmill with air guides, on the one hand is attractive, as it allows to shape the inflow on the rotor blades, and on the other, it is controversial, as it significantly increases the complexity of the structure, and thus increases its cost, which in turn reduces the attractiveness of the solution.

II. NUMERICAL RESEARCH

The publication presents a numerical analysis of the flow and operation of a wind turbine with a vertical axis of rotation, including the determination of the torque and power that can be obtained.

The subject of the analysis has been a structural solution consisting of two elements: a rotor and an air guides ring.

Simulations were carried out for different values of the tip speed ratio and different values of the velocity of the incoming air stream.

As a result of the simulation, the flow through one stage of the wind turbine and the velocity distribution (fig. 1) and pressure distribution in the computational domain were obtained.

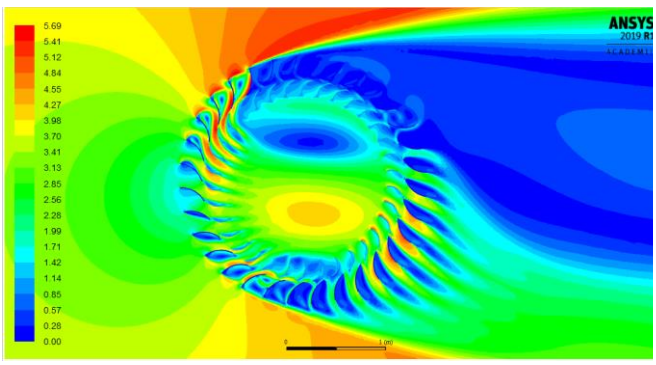

Fig. 1. Velocity contour in the rotor zone

The distribution of the power coefficient (fig. 2) was obtained for different values of the speed factor at different wind speeds.

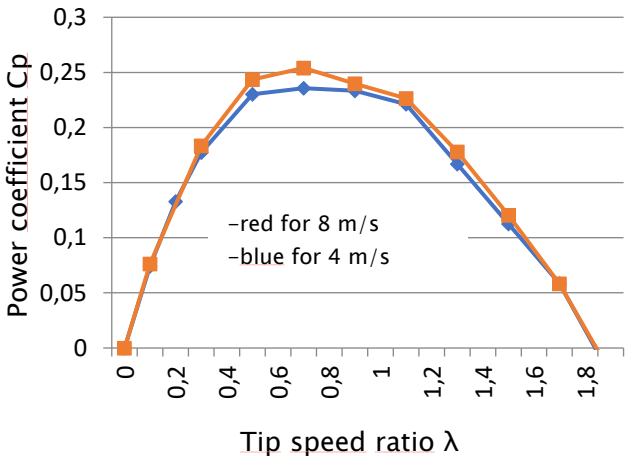

Fig. 2. Dependence of the power coefficient on the tip speed ratio for two wind speed

IV. CONCLUSION

The obtained value of the power coefficient is higher than in classic wind turbines with a vertical axis. The achieved maximum value of the power coefficient was above 25% for the tip spped ratio $\lambda = 0.7$. The conducted analyzes also indicate the possibility of optimizing the proposed design solution in order to increase the efficiency of obtaining energy from wind.

REFERENCES

[1] E. Hau, Wind turbines, Springer, 2006.
[2] R. Green, N. Vasilakos, Energy Policy 2011, 39, 496.
[3] Y. Wicaksono, A. Tjahjana, AIP Conf. Proc. 2017, 1788, DOI:10.1063/1.4968269.
[4] Y. Wicaksono, A. Tjahjana, S. Hadi, AIP Conf. Proc. 2018, 1931, DOI:10.1063/1.5024099.
[5] H.L. Bai, C.M. Chan, X.M. Zhu, K.M. Li, Renew. Energy 2019, 139, 102.
[6] K. Sobczak, D. Obidowski, P. Reorowicz, E. Marchewka, Energies 2020,13, 3717.
[7] S. Leguizamón, F. Avellan, Renew. Energy 2020, 159, 300, DOI:10.1016/j.renene.2020.03.187.
[8] V. Sammartano, G. Morreale, M. Sinagra, A. Collura, T. Tucciarelli, Procedia Eng. 2014, 89, 540, DOI: 10.1016/j.proeng.2014.11.476.

PROBABILISTIC MODELONG OF MECHENICAL CANTILEVER OSCILATOR FLUCTUATION

Petro Kosobutskyy[1], Andriy Zdobytskyi[1], Uliana Marikutsa[1], Mykhaylo Melnyk[1], Marek Iwaniec[2]
Lviv Polytechnik National University
petro.s.kosobutskyi@lpnu.ua, andrii.y.zdobytskyi@lpnu.ua, uliana.b.marikutsa@lpnu.ua, mykhaylo.r.melnyk@lpnu.ua
AGH University of Science and Technology
Iwaniec@agh.edu.pl

ABSTRACT

The dynamics of oscillations of cantilever-type oscillators has been studied. The probabilistic model of the cantilever is explained. The dependences for the probability density, the mean mathematical expectation, and the standard deviation are developed. The fluctuation model of the cantilever is constructed and the dependences for the probability density for the direct problem are developed. Modeling of mathematical expectation and phase variance for the inverse problem is performed.

KEYWORDS: **oscillator, atomic force microscope, probability density, mathematical expectation, variance.**

I. INTRODUCTION

Mechanical oscillators of the cantilever type in the form of a microconsole with one free end have become widely used due to their high quality factor. Their use has greatly simplified the practical implementation of atomic force microscopy, significantly increased the sensitivity of analyzers in biosensors, and the small value of the inertial mass of the cantilever allowed to significantly increase the resonant frequency of sensor fluctuation [1].

Despite the fact that many works have been devoted to the study of the dynamics of cantilever oscillations systems, the corresponding task remains relevant in the future [2]. Sensor probes are exposed to random external actions, so the measured parameters require statistical and probabilistic averaging. So far, this problem has hardly been solved or has been solved for partial cases [3].

II. SUBSTANTIATION OF THE PROBABILISTIC CANTILEVER MODEL

Let us omit the details of substantiation of the cantilever oscillation dynamics under the force applied to the free end [4]. To reveal the main essence of the work, we assume that the unfixed end of the cantilever fluctuates as a system with concentrated parameters - inertia is expressed by the value of the oscillator mass m, and elasticity - a parameter of rigidity μ.

We assume that the integral probability $dF(t \le T \le t+dt) = f(t)dt$ is proportional to the width of the interval, dt:$dF = \kappa \cdot dt$, where the constant coefficient κ can be determined from the rationing condition $\int_0^{2\pi/\omega_0} f(t)dt = \kappa \int_0^{2\pi/\omega_0} dt = 1$, whence $\kappa = \frac{\omega_0}{2\pi}$. Therefore, the probability density function will be the following $f(t) = \frac{2\omega_0}{\pi}$.

This means that the random variable t is evenly distributed. Its probability in the interval $[t_1, t_2]$ is : $F(t_1 \le T \le t_2) = \frac{\omega_0}{2\pi}(t_2 - t_1)$.

The average $\overline{T}$ for the period $2\pi/\omega_0$ is:
$\overline{T} = \int_{-\infty}^{\infty} t \cdot f_T(t) \cdot dt = \frac{\pi}{\omega_0}$,

And the mean $\overline{T^2}$ of the square is $\overline{T^2} = \frac{1}{3}\left(\frac{2\pi}{\omega_0}\right)^2$.

Then, the variance of the random variable is:
$D_T = \overline{T^2} - \left(\overline{T}\right)^2 = \frac{1}{3}\left(\frac{\pi}{\omega_0}\right)^2 > 0$,

And its standard deviation $\sigma_T = \frac{1}{\sqrt{3}}\frac{\pi}{\omega_0}$,

that is, the condition of non-dispersion is satisfied.

The amplitude varies in the interval based on absolute value $[0, y_0]$. Therefore, the average $\overline{Y}$ (mathematical expectation) will be equal to:

$\overline{Y} = \int_{-\infty}^{\infty} y \cdot f_Y(y) \cdot dy = \frac{y_0}{\pi}$,

and the mean of square (intensity):

$\overline{Y^2} = -\frac{1}{\pi}\int_0^{y_0} \sqrt{{y_0}^2 - y^2}\,dy + \frac{2{y_0}^2}{\pi}\int_0^{y_0} \frac{dy}{\sqrt{{y_0}^2 - y^2}}$.

After calculations we obtain the variance of the amplitude:

$D_Y = \overline{Y^2} - \left(\overline{Y}\right)^2 = \frac{{y_0}^2}{2}\left(1 - \frac{2}{\pi}\right)$, that is, the condition of non-dispersion is satisfied. The standard deviation of the amplitude is:

$\sigma_Y = \frac{y_0}{\sqrt{2}}\sqrt{1 - \frac{2}{\pi}}$.

The fluctuation model of the cantilever is constructed following such calculations and [8-9], the dependences for equal distribution of fluctuations phase for the direct problem are developed.

The mathematical expectation modeling and the variance of the oscillation phase is performed for the inverse problem of equal amplitude distribution.

REFERENCES

[1] Berg Voigtlander. Scanning Probe Microscopy. Atomic Force Microscopy and Acanning Tunneling Microscopy. Springer (2015) 382 p.

[2] Mateusz Romaszko, Bogdan Sapiński, Andrzej Sioma. Forced Vibrations Analysis of a Cantilever Beams using the Vision Method. Journal of theoretical and applied mechanic, vol.**53**, 1, pp. 243-254, Warsaw 2015. http://www.ptmts.org.pl/2015-1-romaszko-in.pdf

[3] Zibenko O.S., Tarasevich Yu.Ja. Probability method in mechanics. Kyiv: NTU»KPI».-2016.-240 p.

[4] Haran Dr. Second-order Systems: Vibrating Cantilever Beams. ME 3504 Vibrating Cantilever 2 11 08 05_copy.pdf-STDU Viewer.

SIMULATION MODEL FOR CONVERSION HEAT TO ELECTRICITY UNDER MAGNETIC FLUX BASED ON COMSOL

Oleh Matviykiv[1], Mykhailo Lobur[1], Nataliia Bokla[1], Tamara Klymkovych[1], Serhiy Shcherbovskykh[1]
Lviv Polytechnic National University[1]
nataliia.i.bokla@lpnu.ua, tamara.a.klymkovych@lpnu.ua, serhiy.v.shcherbovskykh@lpnu.ua

ABSTRACT

The paper proposes the model that describes the conversion of heat to electricity under the magnetic flux. The model is based on the finite element method and created using COMSOL. Geometric plate parameters, thermal conditions, and electromagnetic properties of the material are identified. Based on the specified parameters and conditions, the distribution of electric potential in the plate is simulated.

KEYWORDS: **COMSOL, Seebeck effect, finite element method, heat to electricity converting.**

I. INTRODUCTION

Thermal pollution is one of the fundamental problems of today. Large data centers, thermal power plants, cars, and other energy facilities emit large amounts of heat into the environment. Every year, the equipment's total capacity and number are snowballing, so this problem tends to worsen. Such heat is not hot enough to be used for practical purposes. In particular, it is not enough for the efficient operation of the heat engine, and it cannot be transferred over long distances to heat the home. As a result, this heat is released into the atmosphere, exacerbating global warming.

The scientific problem is improving and practical implementation of technology for converting heat into electricity. A low thermal gradient is sufficient for this technology, and the transducers themselves can be minimized to nanoscales. The efficiency of heat conversion into electricity increases by applying an additional magnetic field.

At the initial stage, such technology can be applied to watches, smartphones, and other smart gadgets that charge directly from the human body's heat. In addition, this technology can be used to collect heat dissipated in radiators to increase the energy efficiency of consumer electronics, autonomous vehicles and aircraft, and other ultra-low-power devices used in the IoT. This technology can be used to produce electricity from thermal pollution in the future. Peltier elements carry out the conversion of thermal energy into electricity. An external magnetic field increases the efficiency of this transformation based on Seebeck effect.

The study aims to develop a simulation model based on the finite element method, which describes the conversion of heat into electricity under the action of a magnetic field. This model is planned to be used to compare theoretical results and experimental results [1–3].

II. MODELLING AND SIMULATION

In the COMSOL application package, a simulation model (fig. 1) of the studied phenomena was developed. Three physical interfaces, "Heat Transfer in Solids", "Magnetic Fields No Currents" and "Electric Currents" were used for simulation. Each interface calculates the parameters for a given physical phenomenon during the calculation. Then the computed results are transmitted regarding physical interfaces. Thus, the analyses are performed on the next iteration, taking into account related physics interfaces. The developed model is a square plate with 5 mm x 5 mm x 0.2 mm geometric parameters.

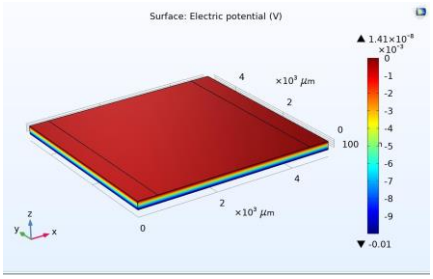

Fig. 1. Electric potential distribution in the plate

The plate material is selected YIG. A thin layer of platinum is sprayed on the opposite edges of the plate. Each platinum layer has geometric parameters of 5 mm x 500 μm x 2 nm. Assume that the ambient temperature is 20 degrees Celsius. Heat with a temperature of 50 degrees Celsius is supplied to the lower part of the plate. As a result, a heat gradient of 30 degrees Celsius was formed between the upper and lower surfaces of the plate. Assume that there is convective heat transfer on the side surfaces of the plate. Perpendicular to the side surface acts magnetic flux with induction 1T.

III. CONCLUSION

The simulation model of conversion of heat to electricity under magnetic flux is developed. Geometric, thermal, and electromagnetic parameters are identified. Using COMSOL electric potential distribution in the plate is simulated.

REFERENCES

[1] J. Woźny, R. Gozdur, B. Guzowski, Ł. Bernacki, "Micromagnetic Simulation of Thermal Generation of Spin Waves Using MuMax3", Acta Physica Polonica A, 2020, 137(5), pp. 737-740, DOI: 10.12693/APhysPolA.137.737

[2] B. Guzowski, R. Gozdur, A. Kociubiński, "Sputtered Y3Fe5O12 Films for Spintronics Application", Acta Physica Polonica A, 136(5), 693-695, 2019, DOI: 10.12693/APhysPolA.136.693

[3] R. Gozdur, B. Guzowski, M. Hasiak, "Impact of the Effects of Sample Geometry and Forms on the Magnetic Properties of NiFeCuMo Alloy", Acta Physica Polonica A, 135(2), 308-312, (2019). DOI: 10.12693/aphyspola.135.308

TESTING AND EVALUATION OF SUCTION CUPS AS A GRIPPING TOOL FOR A MUSHROOM PICKING ROBOT

Petro Shmigelskyi[1], Oleg Bodnar[2], Ihor Farmaha[3]
Lviv Polytechnic National University, Reest, Inc.[1]
petro.i.shmihelskyi@lpnu.ua, petro@reest.io
Reest, Inc.[2]
oleg@reest.io
Lviv Polytechnic National University[3]
ihor.v.farmaha@lpnu

ABSTRACT

The paper describes the approach for the evaluation of suction cups as a gripping tool for a button mushroom picking robot. Thereare presented the test stand designed to hold a mushroom and measure twist torque of suction cups. In the study suction cups withvarious sizes, shapes and materials were tested. Evaluation results and recommendations are described.

KEYWORDS: **robot, mushroom, picking, gripper, suction cup, agriculture, farming, automation.**

I. INTRODUCTION

Button mushrooms farming requires a lot of manual tedious work. Many of the production processes have been automated in the last decades, but the mushroom picking job is still done manually. Pickers work in a tight and moisture environment with a high humidity level. The quality and quantity of a harvest highly depend on the skills of the staff doing the harvesting [1].

The button mushroom picking technique consists of two steps: twist it around a stem and pull it up. In a farm environment, mushrooms are covered with slippery moisture and their skin is sensitive to damage. That is why the mushroom gripping tool is one of the most responsible parts of a picking robot. Applying not enough force leads to an inability to twist a mushroom, otherwise, too much force can damage a mushroom.

In this study suction cups of various sizes, shapes, and materials were tested to evaluate which ones are best suited for button mushroom picking.

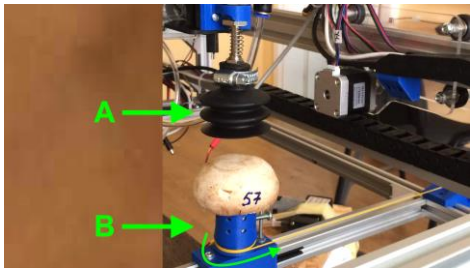

Fig. 1. Suction cup test stand

II. TESTING STAND

The suction cup test stand is created to measure the torque that the suction cup can hold when applied to a mushroom head (Fig. 1). Having the torque measurement allows evaluating suction cups' suitability for twisting action in the picking process.

The test stand consists of a mushroom holder (Fig. 1, B) and a suction cup fixture (Fig. 1, A). A suction cup is installed in the mounting and is pressed to the mushroom head. The same vacuum level -0.76 atm is applied to all tested suction cups. The mushroom holder can rotate around the axel. Torque with increasing value is applied to rotate the holder until the suction cup begins slipping from the mushroom head. The maximum holding torque is recorded as the best parameter for a specific suction cup.

III. RESULTS ANALYSES

About 25 different suction cups were tested in the study. Suction cups with various sizes, shapes, bevels count, material were tested. Experimentally were proven that holding torque (τ) is mostly affected by the inner diameter (*ID*) of a cup. And dependency is close to square function:

$$\tau = f(ID)^2 \quad (1)$$

Flat suction cups with an outer diameter in the range 22-42 mm and the same inner diameter of 9 mm, had similar results in holding torque, which proves that assumption.

Among materials were silicon, rubber, natural rubber, PVC. Also, two cups with foam pad were tested. It was found that material has a small effect on results, in a range of 10%, which is close to the measurement errors [2].

IV. CONCLUSIONS

The best suction cups selected in the study were tested on a real mushroom farm. Even they provided good holding to mushrooms, but they created a circle-shaped bruise on the mushroom skin. With a decrease of vacuum pressure the cup slips and can't twist a mushroom. Experimentally was established that regular suction cups are not suitable for mushroom picking.

REFERENCES

[1] Mark den Ouden, "Mushroom Signals: a practical guide to optimal mushroom growing". ISBN: 9789087401368.

[2] Giacomo Mantriota, Arcangelo Messina, "Theoretical and experimental study of the performance of flat suction cups in the presence of tangential loads", Mechanism and Machine Theory 46(5), May 2011, pp. 607-617.

THE CONCEPT OF USING OF THE UNMANNED AERIAL VEHICLES TO LOCATE POLLUTION SOURCES IN INDUSTRIAL AREAS

Dawid Nowicki, Katarzyna Suder-Dębska, Ireneusz Czajka
AGH University of Science and Technology
dnowicki@agh.edu.pl

ABSTRACT

Miniaturization and development of lightweight energy storage devices have increased the use of UAVs (Unmanned Aerial Vehicles) in technical applications. Continuous development of sensor technology causes the list of UAV applications to grow constantly. This paper presents the application of UAVs to detect pollution sources in an industrial area.

KEYWORDS: **UAV, pollution, photogrammetry, environmental protection, noise pollution.**

I. INTRODUCTION

In the modern world, more and more attention is being paid to the impact that industry has on the environment. Researchers are working on new tools and methodologies to collect information about pollution. Unmanned aerial vehicles are the new tool, that provides the ability to remotely collect information. This paper addresses the topic of opportunities that this new tool provides for the detection of contamination sources.

II. UAV SENSING CAPABILITIES

Human technical activity, in addition to the benefits it creates, is also a source of many types of pollution. Noise emitted by technological equipment is the one type of pollution, but it could also be the information on some malfunction in machinery. Industrial sites always occupy large areas and it is difficult to determine the exact location of the main noise source with the traditional measuring method. The UAV equipped with an array of microphones, and with the support of appropriate signal processing is capable of producing the sound map, which is the representation of sound intensity distribution on the assessed area. With the help of computer vision software, UAVs are able to collect images of the surveyed area and produce the sound map on their own, without the need to provide external maps. The maps generated from images collected in sight can carry information about another type of pollution, which is air pollution caused by combustion. Solid particles which are the effect of unclean burning affect settle near where they are emitted from. Winter seasons increase heating demand, which easily translates into more sources of potential pollution. The presence of snow, however, increases the possibility of detecting the presence of solid particles deposited on the surface.

III. PHOTOGRAMMETRY

To provide the ability of producing maps with the use of UAV the photogrammetry technics are used. The vehicle collects photographs of the terrain below, and next, in the process of combining them together the representation of a surveyed area is generated. The way the photos are taken over the terrain affects the processing time and the quality of the final product. Research on the influence of three parameters of the image acquisition process on the computation time and the digital surface model accuracy has been conducted. Control variables examined during the study were the level of transverse overlap of photos, the level of longitudinal overlap of photos, and the flight height above the photographed terrain. The study was conducted in a specially prepared environment for taking aerial photographs of the terrain. There were conducted 32 experiment simulations. Images were processed in WebODM photogrammetric software to produce digital surface model of photographed terrain, which then were compared with the original model by measuring the position of specially introduced ground control points. The errors and the time needed to process photos from each experiment were compared, to choose the set of variables that gives the most accurate result in terms of the time required to generate.

IV. FUTURE WORK

There are carried out the works on the implementation of a microphone array into the UAV. This provides the ability of sensing of the acoustic signal. Acoustic signal acquisition by UAV in conjunction with photogrammetry will provide the ability to produce the acoustic maps of a surveyed terrain, which are the essential element to locate pollution sources such as an excessive sound intensity level or the furnaces that pollute the atmosphere with solid particles.

V. CONCLUSION

UAV are used in many different applications. This is relatively new tool, and the list of utilization is constantly growing. Environmental protection is an area in which the use of UAV will provide the access to information that is not available through the standard measurement methods.

REFERENCES

[1] K. Suder-Dębska, I. Czajka, A. Gołaś, "Modelowanie rozkładu pola akustycznego wokół wiertni przy poszukiwaniu I eksploatacji gazu łupkowego", Materiały XX Konferencji Inżynierii Akustycznej I Biomedycznej, Zakopane, 2013.

[2] A. Gołaś, I. Czajka, K. Suder-Dębska et al. "Mechanical engineering in smart grid technology", Wydział Inżynierii Mechanicznej I Robotyki AGH, Kraków, 2015.

[3] T. Yamada, K. Itoyama, K. Nishida et al. "Sound source tracking using multiple microphone arrays mounted to an Unmanned Aerial Vehicle", Sound Source Tracking by Drones with Microphone Arrays, pp. 796-801, 2020.

[4] T. Ohata, K. Nakamura, A. Nagamine et al. "Outdoor sound source detection using a quadrocopter witch microphone array", Journal of Robotics and Mechatronics, pp 177-187, 2017

TOPOLOGICAL OPTIMIZATION PARAMETERS OF BLADES OF WIND TURBINES

Krzysztof Pytel[1], Andriy Zdobytskyi[2], Mykhaylo Lobur[2], Roman Panchak[2], Anna Hnatiuk[2]
AGH University of Science and Technology[1]
kpytel@agh.edu.pl.
Lviv Polytechnic National University[2]
andrii.y.zdobytskyi@lpnu.ua., mykhaylo.v.lobur@lpnu.ua., roman.t.panchak@lpnu.ua., anna.hnatiuk.knm.2019@lpnu.ua.

ABSTRACT

This paper considers the possibility of modernization and improvement of the wind turbine blade design by the method of topological optimization taking into account the wind load vector while preserving its functional properties. The design of the wind turbine blade has been automatically generated based on geometric limitations of the shape and minimization in terms of weight and maximum rigidity using the algorithm of topological optimization of the software environment Inventor Nastran.

KEYWORDS: **topological optimization, blade, wind turbine, stiffness, material minimization, wind load.**

I. INTRODUCTION AND RESEARCH OBJECTIVE

The development of alternative energy sources, namely wind energy, is undoubtedly an important area for the implementation of energy systems. Modern wind turbines are bulky structures that can only work properly in a narrow area of wind load. However, under the influence of variable wind load, the blades of the wind turbine are deformed, which leads to a decrease in its efficiency [3].

The gradual development of composite materials opens up new ways to use them in fundamentally new industries and aspects. Due to such properties as increased strength, corrosion resistance, and lightweight, composite materials are gradually gaining popularity in the wind energy industry.

The rapid development of new technologies and models of additive production, namely the introduction of new design techniques contributes to the production of various elements of complex geometric shapes. In turn, the generation of structures using the methods of topological optimization and generative design significantly expands their functionality [1]. Due to the creation of lightweight matrix structures of the blades, proper geometric, fatigue, shock, and wear resistance parameters are provided by the action of wind load.

II. MAIN RESULTS AND THEIR DISCUSSIONS

Computer-aided CAD modeling and CAE engineering analysis with appropriate modules of topological optimization and design will be used to check the adequacy of the described assumptions in order to increase the strength of wind turbine blades by topological optimization methods, [2].

At the initial stage of design, we will create a three-dimensional model of the wind turbine blade and investigate it for stresses and strains arising under the action of wind load 380 Pa. Since the classical method of topological optimization is based on the finite element method, the density of the material varies from 0 to 1 at each given optimization point.

The design limitations on volume particle minimization (COMPVF) and additive layer fabrication preparation (TOPTMANCONSTR) are to be set for automatic generation of topology optimization (TOPGEN) by the linear static analysis of the stress-strain state of the (TOPTMANCORD). We also indicate the planes of symmetry of the constraints and the direction of extrusion, in Fig. 1.

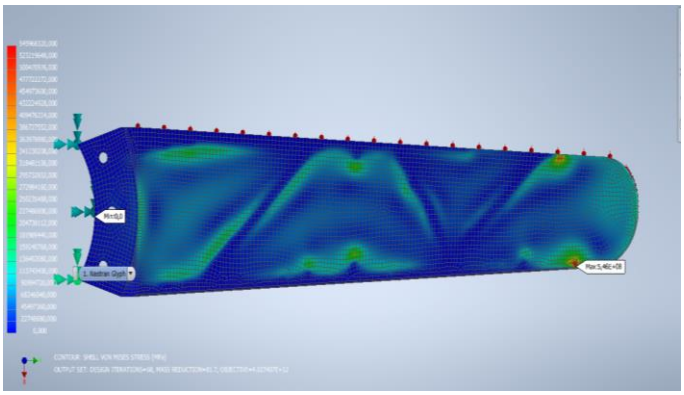

Fig. 1. Automatically generated structure of wind turbine blades

III. CONCLUSIONS

Implementation of the algorithm for topological optimization of the Inventor Nastran environment solves multi-purpose design problems that are intuitively difficult to predict. The structure of the wind turbine blade is automatically generated, which ensures the maximum possible rigidity and minimization of the material by the action of the wind load vector.

REFERENCES

[1]. Meng, L., Zhang, W., Quan, D. *et al*. From Topology Optimization Design to Additive Manufacturing: Today's Success and Tomorrow's Roadmap. *Arch Computat Methods Eng* 27, 805–830 (2020). doi.org/10.1007/s11831-019-09331-1.

[2]. Zdobytskyi, M. Lobur, R. Panchak, R. Sika and K. Kalinowski, "Increasing the Strength of Materials by Topological Optimization Methods," *2021 IEEE 16th International Conference on the Experience of Designing and Application of CAD Systems (CADSM)*, 2021, pp. 6-9, DOI: 10.1109/CADSM52681.2021.9385222.

[3]. Ying Ma, Shengli Xu, Haitao Liu, Xiaofang Wang Optimization of Reinforcing Ribs of a Hollow Fan Blade Using Metamodel-Based Optimization Algorithm Conference: Proceedings of ASME Turbo Expo 2016: Turbine Technical Conference and Exposition June 2016. DOI:10.1115/GT2016-57226

TRAM NOISE LEVEL DETERMINATION ANALYSIS CASE STUDY FROM LVIV

Mariia Orynchak, Volodymyr Havran, Mykhaylo Melnyk
Lviv Polytechnic National University[1]
mariia.r.orynchak@lpnu.ua., volodymyr.b.havran@lpnu.ua., mykhaylo.r.melnyk@lpnu.ua

ABSTRACT

The tram noise level determination analysis case study from Lviv city is being researched and developed. The experimental measurements were compared to the most recent ISO tram noise measurements. The obtained data revealed that the noise exceeded up to 2x times. The findings indicate that when developing new standards for noise emission levels, we must consider the tram itself as a noise load centre. The final updated standard will pay attention to future studies, taking into account paved coverage, tram longevity, public transportation station, and the distance from the noise source to its scattering through surrounding buildings.

KEYWORDS: **noise, noise emission, traffic noise, tram noise, acoustics.**

I. INTRODUCTION

Global environmental issues are caused by traffic noise loads, which influence the rhythms of towns and cities. The noise loads can be reduced after creating a unified tailor-made model for specific places of living. Some cities suffer only from car traffic noise, but UNESCO cities struggle with heavily loaded acoustics from trams, particularly on paved ground coverage. They amplify the sound's impact. The current scientific paper aimed to break the dependencies and find the golden mean for tram noise level determination analysis, based on the Lviv city example. We already know that there exists an adapted model for noise load measurement, established on experimental data. To estimate the noise load, measurements can be made using appropriate instruments. However, when the task arises to build a noise map, it is necessary to use forecasting methods based on the number of rail vehicles that have passed and their type[1].

Determination of noise levels in train station zones is based on the preparation of analysis models, which is a very demanding procedure because of a multitude of parameters that have to be collected in the process[2]. Noise emission and absorption conditions are quite complex because of: a great number of various sources and factors influencing the occurrence and spreading of noise, different types of rail vehicles, a great number of rail systems and turnouts, different permanent way structures, dense construction in the surrounding areas, etc. [3]

The examination of traffic noise levels in such metropolitan environments necessitates the observance of a number of criteria that are not relevant when analyzing traffic noise in rural areas. For example, in metropolitan road and railway traffic corridors, traffic conditions and flow rates are very variable, with frequent variations in vehicle movement speeds. In [4] the authors performed a detailed description and analysis of some of the most used TNMs, first presenting the historical development of the earliest models and then focusing on some countries' adopted models.

Given the time required to create a noise model and conduct noise level calculations, as well as the volume of data to be processed, it is easy to assume that the problem areas of greatest concern are train stations and the zones surrounding them. Because of the large number of different sources and factors influencing the occurrence and spread of noise, different types of rail vehicles, a substantial percentage of rail systems and turnouts, different permanent way structures, dense construction in the surrounding areas, noise emission and absorption conditions are quite complex.

II. COLLECTION INPUT DATA

Number of trams and cars is increasing. This situation provides high load traffic in Lviv city, so we decided to investigate noise in two main streets in Lviv city. First street was Shevchenka St, 22 and second street was Lychakivska St, 89. We measured the noise level with a specialized device for a whole day. Both streets showed high noise level load in time ranges without traffic jams. Figure 1 shows Street noise level based on time ranges.

All this data allows us to make and modernize the analysis of noise load.

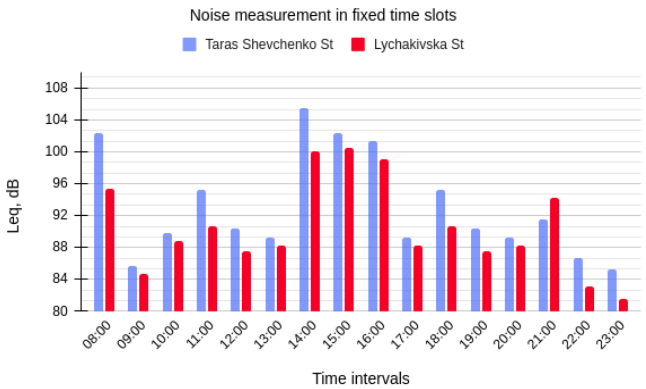

Fig. 1. Noise measurement in Lviv city

III. NOISE DETERMINATION

In 2012 Ministry for Communities and Territories Development of Ukraine approved new rules cased to the noise level in Ukraine. Based on the new noise standards described in DBN B.2.6-XX:201X allowed noise level in streets where citizens can live should be in range of 40 - 55 dB[5].

Investigations which we made previously showed that the real situation is not so good and does not reply to government standards. After exploring problem areas we can provide improvements based on the new types of rails and their installation to the road which will improve existing noise level situations and will decrease noise level in selected street areas.

IV. Conclusion

While making experimental measurements, the case study investigated that input collected data from 3 noise centre streets with heavily packed traffic the sound norms are exceeded in X times which causes noise dissipation at a distance of up to 5 meters. For getting the ability to create Traffic Noise predictive Models (TNMs) which are often used in order to predict and/or monitor road traffic noise impact on the environment. In general, a logarithmic function is assumed, and the fit parameters are assessed and utilized to estimate the noise level for any traffic flow[6]. Because the parameters are evaluated on data obtained in that specific place and conditions, this approach produces a form of "site bias" in the forecast.

To reduce tram traffic noise and the vibration is a widely used concept for improving the life standard in the vicinity of railway lines. Elevated levels of noise and vibration are the main factors of dissatisfaction, especially in urban areas.

The strong dependence on the site, and consequently on the vehicle flow volume and typology, will be sketched for future forecasting, together with the influence of climatic parameters and ground coverage type.

References

[1] Maria Orynchak; Mykhaylo Melnyk; Volodymyr Havran, Methods for Forecasting the Noise Level of Rail Vehicles, 2021, DOI: 10.1109/DIPED53165.2021.9552324

[2] Stjepan Lakušić, Vesna Dragčević, Maja Ahac, Saša Ahac (2011). Determination of noise levels in railway station zones. Croatia, Gradevinar, p.521, UDK 656.211.001.5:699.844

[3] Wölfel et al.: AR INTERIM CM, Adaptation and revision of the interim noise computation methods for the purpose of strategic noise mapping, WP 3.1.1: Road traffic noise - Description of the calculation method, 2002.

[4] Quartieri J., Mastorakis N. E., Iannone G., Guarnaccia C., D'Ambrosio S., Troisi A., Lenza T.L.L, A Review of Traffic Noise Predictive Models, Proc. of the 5th WSEAS Int. Conf. on "Applied and Theoretical Mechanics" (MECHANICS'09), Puerto De La Cruz, Canary Islands, Spain, December 14-16, 2009. ISBN: 978-960-474-140-3 / ISSN: 1790-2769, pp. 72-80.

[5] https://dbn.co.ua/load/normativy/dbn/1_1_0_1078

[6] R.T. Sooriyaarachchi, Development of a Road Traffic Noise Prediction Model, B.Sc. Thesis, Department of Physics, University of Colombo, 2005

USE OF CELLULAR AUTOMATA IN MODELING HEAT AND MOISTURE CONDUCTIVITY PROCESSES AT THE MATERIAL BOUNDARY

Yaroslav Sokolovskyy[1], Oleksiy Sinkevych[2]
Department of Computer-Aided Design Systems, Lviv Polytechnic National University [1]
sokolowskyyyar@yahoo.com
Department of Information Technology, National Forestry University of Ukraine [2]
oleksiy1694@gmail.com

ABSTRACT

In this paper, we modeled the processes of heat and moisture transfer at the material boundary using cellular automata. The proposed cell-automatic model contains local relationships between cells that describe their behavior. We can also specify the physical characteristics of the material in the model, including its temperature and humidity. The proposed algorithm for the use of cellular automata allows to obtain a reliable result without the need for expensive and complex practical experiments. To speed up the calculation process, we used multilayer, which consists in obtaining numerical values of the physical characteristics of the material from several adjacent cells that interact on the same coordinate.

KEYWORDS: **cell-automatic model, temperature, humidity, algorithm, multilayer**.

I. INTRODUCTION

Differential equations are often used to solve problems of numerical modeling of dynamic systems, which contain complex boundary and initial conditions, as well as materials with nonlinear parameters, the implementation of which requires significant resources of the computer system and time. For this reason, it is proposed to use new approaches to solving this class of problems. These approaches include the method of cellular automata (CA) [1]. This method allows to describe and determine changes in the physical characteristics of the material [2]. In addition, CA models allows to set rules of conduct for each element of the system [3]. This in turn allows to use them in mathematical modeling of various physical phenomena and processes, including heat and moisture conductivity processes.

II. ALGORITHM FOR USING CELLULAR AUTOMATA

The studied 3D model is a lumber of fixed size. This model is presented as a set of cells (Fig. 1), where *Pi* is the point of a cell, and its index "*i*" can take the following values: "*a*" is the point of the wood drying agent, "*b*" is the point located on boundaries of wood, "*m*" is a point belonging to wood, and "*tmp*" is a point for storing temporary values.

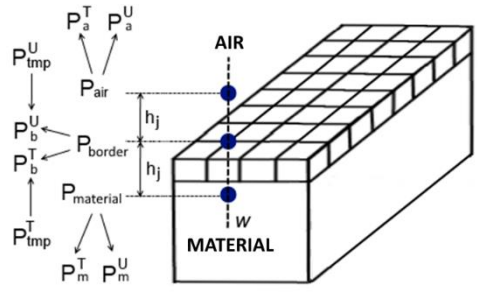

Fig. 1. Scheme of using CA model on the material surface

When we use this scheme, the upper point-marking indexes (P^T,P^U) are responsible for numerical temperature and humidity values at this point. In addition, the new values $P_b{}^U$ and $P_b{}^T$ we save only after checking the intermediate values $P_{tmp}{}^U$ and $P_{tmp}{}^T$, which are defined as follows:

$$\begin{cases} P_{tmp}{}^T = \dfrac{P_a{}^T(C_3 - C_2 - C_1\delta) + P_m{}^T(C_5 - C_4) - C_1(P_m{}^U - P_a{}^U)}{C_3 + C_5 - C_2 - C_4 - C_1\delta} \\ P_{tmp}{}^U = \dfrac{C_6(P_m{}^T - P_{tmp}{}^T) + a_j P_m{}^U + C_7 P_a{}^U}{a_j + C_7} \end{cases} \quad (1)$$

Where: $\delta = f(U_m, T_m)$ is thermogradient coefficient, $a_j = f(U_m, T_m)$ are coefficients of moisture conductivity (m^2/s). In this case, the coefficients C_1-C_7 are defined as follows:

$$\begin{array}{lll} C_1 = a_j\rho_0(1-\varepsilon)\beta & C_3 = \beta\lambda_j & C_5 = \alpha\beta h_j \\ C_2 = (a_j\lambda_j)/h_j & C_4 = \alpha a_j & C_6 = a_j\delta \end{array} \qquad C_7 = \beta h_j \quad (2)$$

Where: ρ_0 is basic wood density (kg/m^3), $\varepsilon = f(\rho_0)$ is coefficient of phase transition, $\beta = f(v, T_c, \varphi)$ is moisture exchange coefficient (m^2/s), $\lambda_j = f(U_m, T_m)$ are thermal conductivity coefficients ($W/(m^2\,°C)$), $\alpha = f(T_c, v)$ is a heat exchange coefficient ($W/(m^2\,°C)$), h_j is a displacement step at a given coordinate x, y or z (m).

If we use multilayer to determine the internal numeric values of T_m, U_m in wood, we can determine intermediate values $P_{tmp}{}^U$ and $P_{tmp}{}^T$ as follows:

$$\begin{cases} P_{tmp}{}^U = P_m{}^U - C_1\left(\frac{1}{6}P_{m+3}{}^U + \frac{1}{3}P_{m+2}{}^U + \frac{1}{2}P_{m+1}{}^U - 2P_m{}^U + \right. \\ \quad + \frac{1}{2}P_{m-1}{}^U + \frac{1}{3}P_{m-2}{}^U + \frac{1}{6}P_{m-3}{}^U + \delta\left(\frac{1}{6}P_{m+3}{}^T + \frac{1}{3}P_{m+2}{}^T + \right. \\ \quad \left. \left. + \frac{1}{2}P_{m+1}{}^T - 2P_m{}^T + \frac{1}{2}P_{m-1}{}^T + \frac{1}{3}P_{m-2}{}^T + \frac{1}{6}P_{m-3}{}^T\right)\right) \\ P_{tmp}{}^T = P_m{}^T + C_2\left(\frac{1}{6}P_{m+3}{}^T + \frac{1}{3}P_{m+2}{}^T + \frac{1}{2}P_{m+1}{}^T - 2P_m{}^T + \right. \\ \quad \left. + \frac{1}{2}P_{m-1}{}^T + \frac{1}{3}P_{m-2}{}^T + \frac{1}{6}P_{m-3}{}^T\right) + C_3\left(P_{tmp}{}^U - P_m{}^U\right) \end{cases} \quad (3)$$

The coefficients C_1-C_3 are defined as follows:

$$C_1 = \frac{a_j\Delta t}{h_j{}^2} \quad C_2 = \frac{\lambda_j\Delta t}{c_m\rho_m h_j{}^2} \quad C_3 = \frac{\varepsilon\rho_0 r}{c_m\rho_m} \quad (4)$$

Where: Δt is the time step (s), c_m is specific heat capacity of wood ($J/kg\,°C$), ρ_m is wood density (kg/m^3), r is specific heat of vapor formation (kJ/kg).

To determine the numeric values T_c and φ, when we use CA, it is also necessary to determine the intermediate values ${P_{tmp}}^T$ and ${P_{tmp}}^U$. These values can be defined as follows:

$$\begin{cases} {P_{tmp}}^T = {P_a}^T + \dfrac{C_1({P_b}^T - {P_a}^T)}{C_2} \\ {P_{tmp}}^U = {P_a}^U + \dfrac{C_3({P_b}^U - U_p)}{C_4} - \dfrac{{P_a}^U(P_n - P_s)}{C_5{P_a}^T} + \\ + \dfrac{{P_a}^U P_s {P_{tmp}}^T}{C_5({P_a}^T)^2} - \dfrac{{P_a}^U P_s}{C_5{P_a}^T} \end{cases} \quad (5)$$

where: $P_n = f({P_{tmp}}^T)$ is the new value of pressure of saturated vapor $P_s(kPa)$. In this case, C_1-C_5 are defined as follows:

$$C_1 = \alpha h_j \qquad C_3 = a_j \rho_0 h_j \qquad C_5 = h_g \rho_s \quad (6)$$
$$C_2 = v c_c \rho_c h_g \qquad C_4 = v \rho_s h_g$$

When we use CA, there is an interaction between adjacent cells, which can be described by the following transition rules:

IF P_b, ${P_a}^+$, ${P_a}^-$ **THEN** ${P_{tmp}}^T$ and ${P_{tmp}}^U$ calculate **by** Eq. 1
IF P_m, ${P_m}^+$, ${P_m}^-$ **THEN** ${P_{tmp}}^T$ and ${P_{tmp}}^U$ calculate **by** Eq. 3
IF P_a, ${P_a}^+$, ${P_b}^-$ **THEN** ${P_{tmp}}^T$ and ${P_{tmp}}^U$ calculate **by** Eq. 5
IF ${P_{tmp}}^T > {T_c}^0$ **THEN** ${P_{tmp}}^T = {T_c}^0$
IF ${P_{tmp}}^T < {T_m}^0$ **THEN** ${P_{tmp}}^T = {T_m}^0$

III. Analysis of the Obtained Results

To check the performance of the proposed algorithm, we conducted an experiment in the developed software application [4]. The input data for the experiment we took from the work [5]. As a result, we received graph of changes the temperature and the moisture content of the material (Fig. 2).

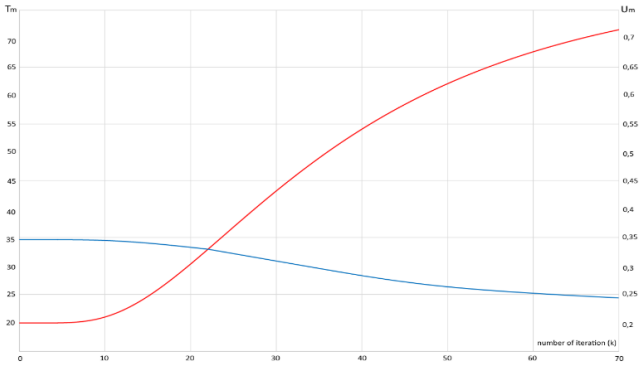

Fig. 2. Graph of changes the temperature and the moisture content of the material in time

Also we received graph of changes the temperature and relative humidity of the wood drying agent (Fig. 3).

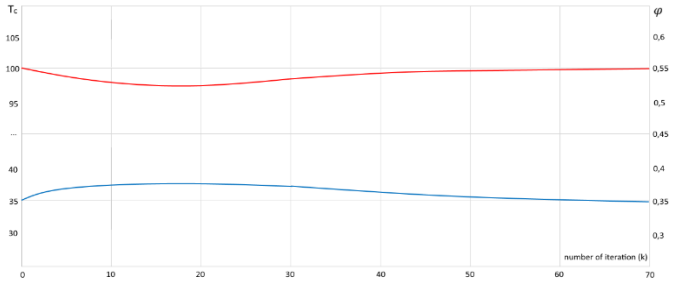

Fig. 3. Graph of changes temperature and relative humidity of the wood drying chamber in time

In addition, we received a graph that reflects changes in temperature and humidity on the material surface (Fig. 4).

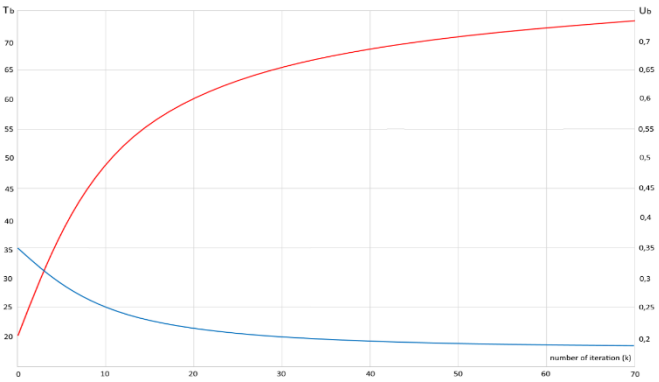

Fig. 4. Graph of changes temperature and humidity on the material boundary in time

To verify the adequacy of the results, we determined the relative error between the obtained results and the results that given in the work [5]. The largest values of relative error were recorded at the beginning of the experiment (Fig. 5). Average value of errors doesn't exceed 7% for T_m and 4.4% for U_m.

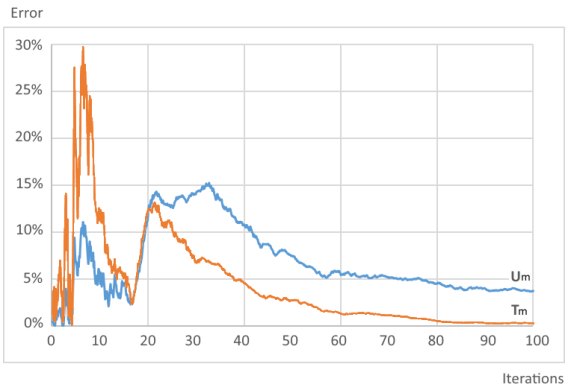

Fig. 5. Graphical representation of the relative error for T_m and U_m

IV. Conclusions

As a result of this work, we obtained results with a low value of relative error. The largest values of this error are present at the beginning of the simulation and are almost absent at the end of the simulation. The average value of this error doesn't exceed 7%. This indicates that the proposed algorithm for using the CA model really allows to successfully solve the problems of heat and moisture transfer at the boundary of the material.

References

[1] D.S. Svyetlichnyy, Modeling of the microstructure: From classical cellular automata approach to the frontal one. Comput. Mater. Sci., vol. 50, pp. 92-97, 2010.

[2] S. Bandini and M. Magagnini, Parallel Processing Simulation of Dynamic Properties of Filled Rubber Compounds Based On Cellular Automata. Parallel Comput., vol. 27, pp. 643-661, 2001.

[3] M. Sitko, Q. Chao, J. Wang, K. Perzynski, K. Muszka, and L. Madej, A parallel version of the cellular automata static recrystallization model dedicated for high performance computing platforms. Development and verification. Comput. Mater. Sci., vol. 172, pp. 109–283, 2020.

[4] Ya. Sokolovskyy, O. Sinkevych, and R. Voliansky, Development the software for simulation of physical fields in wood drying chambers by using cellular automata. Materials of the XV International Conference CADSM'2019, Lviv Polytechnic Publishing House, pp. 24-27, 2019.

[5] Ya. Sokolovskyy, O. Sinkevych, and R. Volianskyi, The study of cellular automata method when used in the problem of capillary-porous material thermal conductivity. Advances in Intelligent Systems and Computing V: Springer Computer Science, vol. 1293, pp. 714–729, 2020.

VISUALIZATION TOOL FOR ROOM MODEL SIMULATION AND WALL ROUGHNESS ANALYSIS

Mykhailo Muliar, Roman Habovskyi, Mykhaylo Lobur, Mykhaylo Melnyk, Pavlo Denysiuk
Lviv Polytechnic National University
mykhailo.muliar.knm.2018@lpnu.ua, roman.habovskyi.knm.2018@lpnu.ua, Mykhaylo.V.Lobur@lpnu.ua

ABSTRACT

The article proposes a method of visualizing the geometry of the room. The developed method made it possible to build models ofrooms for further analysis and use in 3D-processing systems.

KEYWORDS: **3D model, MATLAB, point cloud, 3D scanner.**

I. INTRODUCTION

Today on the market you can find a large number of 3D scanners of rooms, which allow you to get a model of the room and evaluate the characteristics of surfaces. Based on the obtained data, it is possible to assess the optimal lighting conditions and acoustic quality of the rooms. One of the leaders in the production of 3D scanners is EinScan [1], whose products are quite expensive. Therefore, it was decided to develop an alternative for a 3D scanner based on a laser rangefinder. To process the aggregate data from the rangefinder, the task is to develop a method and programmatically implement it.

II .DEVICE DATA PRE-PROCESSING

The device returns many points in a spherical coordinate system. On the basis of which you want to present a model. There are two common methods of presenting a digital model - in the form of an irregular grid - triangulation (TIN-surface) and regular grid (GRID-surface) [2]. If the first option allows you to more accurately describe any element of the surface, the second is used to treat the resulting surface by different methods [3].

Since the device detects points with a constant angular pitch, the result is data that is easy to represent as a GRID surface.

Because the device returns a cloud of points in a spherical coordinate system, they are converted into a Cartesian coordinate system according to the following formula [4]:

$$\begin{cases} x = r\sin\theta\cos\varphi, \\ y = r\sin\theta\sin\varphi, \\ z = r\cos\theta. \end{cases} \quad (1)$$

III .DATA VISUALIZATION IN THE MATLAB SYSTEM

To determine the geometric properties of the surface, it is proposed to perform local regression [5] of the plane along both axes of the surface. As a result, you can get an image of the surface of the plane and the cloud of points on the basis of which it was built. In fig. 1 shows the visualization of one of the surfaces (walls) of the room in the MATLAB system.

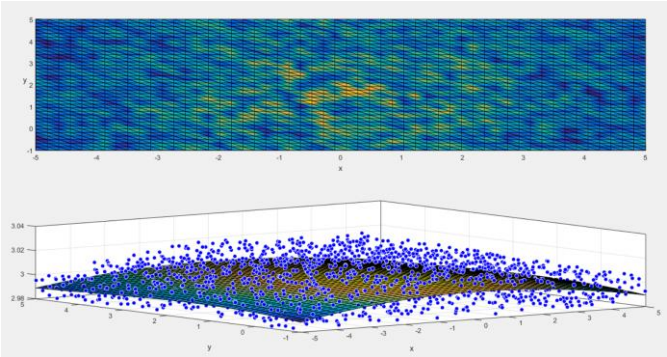

Fig. 1. Visualization of the built-in surface and its regression

IV. MODEL PARAMETERS

The approximated plane allows to reduce the effect of measurement error, as well as to obtain the standard deviation of the cloud of points from it.

After approximating each of the surfaces, we get the opportunity to further measure the difference between distances and angles between the walls, as a result of building a model of the room.

V. CONCLUSIONS

A method has been developed that has made it possible to process and visualize data obtained from a laser rangefinder. The software implementation of the proposed solutions made it possible to build a model of the room for further study of its geometric characteristics.

To increase the accuracy of the model, it is proposed to divide the cloud of surface points into several sets that will describe its different areas.

REFERENCES

[1] Salvatore Barba, Sara Morena, SHINING 3D EINSCAN-PRO, application and validation in the field of Cultural Heritage, from the Chillida-Leku Mus. The International Archives of the Photogrammetry, Remote Sensing and Spatial Information Sciences, Volume XLII-2/W18, 2019. Optical 3D Metrology, 2–3 December 2019, Strasbourg, France.

[2] R.Y Ripetsky, V.M Senychak, Interpolations of spatial data based on surfaces for software of geographic information systems (GIS), Prykarpattya Bulletin NTSh. Numeric. - 2011. - 274 - 276 s.

[3] Magnuszewski A. GIS w geografii fizycznej. Wyd. naukowe PWN. – Warszawa, 1999. – 187 s.

[4] Marina Radchuk, Application of some orthogonal coordinate systems in solving problems, 2014. - 14 s.

[5] Abdul Nurunnabi, “Robust locally weighted regression for ground surface extraction in mobile laser scanning 3d data”.

WAYS TO INCREASE THE EFFICIENCY OF THE LIDAR SCAN SYSTEM OF THREE-DIMENSIONAL OBJECTS

Khranovskyi Mykola, Yusiuk Vladyslav, Andriy Zdobytskyi, Tamara Klymkovych, Uliana Marikutsa[1]
mykola.khranovskyi.mknit.2021@lpnu.ua., vladyslav.yusiuk.mknit.2021@lpnu.ua., uliana.b.marikutsa@lpnu.ua, andrii.y.zdobytskyi@lpnu.ua., tamara.a.klymkovych@lpnu.ua.
Lviv Polytechnic National University, CAD Systems Department,

ABSTRACT

The article discusses the features of using lidars as devices for scanning three-dimensional objects. A comparative analysis of different types of optical, acoustic and laser devices is carried out, based on which ways to increase the efficiency of laser scanning technologies are proposed. The structural scheme of technical realization of lidars with the use of cloud services is developed.

KEYWORDS: **laser, cloud of points, API, lidar, radar, scanning, 3D.**

I. INTRODUCTION AND RESEARCH OBJECTIVE

Modern 3D-scanners are high-tech devices, the main purpose of which is to reproduce three-dimensional models of various physical objects of appropriate shape and size. 3D scanners accurately measure the linear dimensions, determine any object's geometric shape, and then create a three-dimensional digital model.

Different types of 3D scanners are used to perform such work. The most common are radars: optical and acoustic. Complex objects require the use of lasers, as they make it possible to reproduce complex objects with high accuracy. However, these systems are quite complex and expensive..

II. MAIN RESULTS AND THEIR DISCUSSIONS

Laser 3D scanners (Lidars) consist of components responsible for determining distance, positioning, spatial orientation, creating a cloud of points, and the signal emitter and receiver. [1]

The distance determination system consists of a laser and a spectrum analyzer. The laser creates and sends a light flux that returns to the receiver. Also, the laser simultaneously sends a signal to the database to create a timestamp, which is used to compare the information provided by the receiver.

The reflected signal enters the spectrum analyzer. Together with the wavelength, time of signal reception and angle of refraction, the information is transmitted to the database, where it is grouped and compared. The database also receives information from the GPS unit on the location, position and dynamics of the system. The entire flow of information is stored in the database, which creates an array of points of the object of varying complexity [2, 3].

Since creating an array of data requires significant resources for processing and storage of data, it is rational to take advantage of the unlimited possibilities of cloud services. Thus, the system receives many benefits. It is more profitable to use cloud capacities than to keep your own ones. Such storage gives users instant access to a wide range of resources and applications hosted in another organization's infrastructure through a web service interface. They can significantly simplify the requirements for the system, and increase user usability in combination with the mobile application. Cloud storage services can be accessed via a web service interface (API) or applications that use an API. The algorithm of the system is shown in Fig. 1.

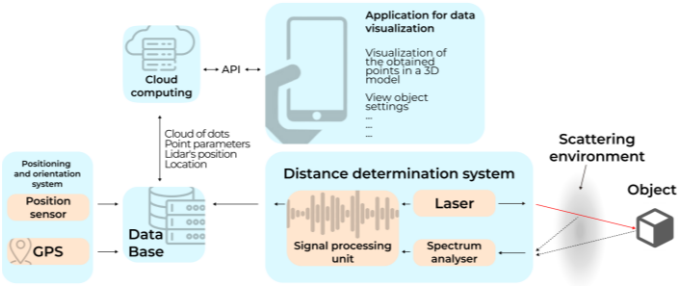

Fig. 1. Block diagram of technical implementation of leaders using cloud technologies.

III. CONCLUSION

The implementation of the system has a number of significant advantages over cloud storage. Moreover, it provides users with instant access to a wide range of resources and applications hosted in another organisation's infrastructure via the interface of the Web service. The use of an API significantly increases the usability of the system, as the user is provided with the necessary access to the results via a mobile application for instant viewing at any convenient time.

REFERENCES

[1] Mehendale N. Review on Lidar Technology [Електронний ресурс] / N. Mehendale, S. Neoge // K. J. Somaiya college of Engineering. 2020. https://papers.ssrn.com/sol3/papers.cfm?abstract_id=3604309.

[2] McManamon. LiDAR technologies and systems / McManamon, Paul F.. Bellingham, Washington, USA: SPIE, 2019. 40 c. (Society of Photo-Optical Instrumentation Engineers). (ISBN 9781510625396).

[3] Zdobytskyi, M. Lobur, V. Dutka, M. Prodanyuk and O. Senkovych, "Determination of Dispersion Medium Parameters by Intelligent Microelectromechanical System," 2020 IEEE XVIth International Conference on the Perspective Technologies and Methods in MEMS Design (MEMSTECH), 2020, pp. 49 52, doi: 10.1109/MEMSTECH49584.2020.9109482.

INDEX

For Notes

Наукове видання

САПР у проектуванні машин.
Питання впровадження та навчання

Матеріали
XXIX Міжнародної польсько-української науково-технічної конференції

Під патронатом ректора Гірничо-металургійної академії імені Станіслава Сташиця професора Єжи Ліса

Відповідальний за випуск – к. т. н., доцент Здобицький А.Я.

Підписано до друку 29.12.2021
Формат 60×84 1/8. Папір офсетний. Друк офсетний
Умовн. друк. арк. 4,7. Обл.-вид. арк. 2,6
Наклад 30 прим. Зам. 211586

Видавець і виготівник: Видавництво Львівської політехніки
Свідоцтво суб'єкта видавничої справи ДК № 4459 від 27.12.2012 р.

вул. Ф. Колесси, 4, Львів, 79013
тел. +380 32 2584103, факс +380 32 2584101
vlp.com.ua, ел. пошта: vmr@vlp.com.ua